Accepted Manuscript

Indolinone-based acetylcholinesterase inhibitors: synthesis, biological activity and molecular modeling

Hamidreza Akrami, Bibi Fatemeh Mirjalili, Mehdi Khoobi, Hamid Nadri, Alireza Moradi, Amirhossein Sakhteman, Saeed Emami, Alireza Foroumadi, Abbas Shafiee

PII: S0223-5234(14)00048-8

DOI: 10.1016/j.ejmech.2014.01.017

Reference: EJMECH 6670

To appear in: *European Journal of Medicinal Chemistry*

Received Date: 31 August 2013

Revised Date: 7 January 2014

Accepted Date: 9 January 2014

Please cite this article as: H. Akrami, B.F. Mirjalili, M. Khoobi, H. Nadri, A. Moradi, A. Sakhteman, S. Emami, A. Foroumadi, A. Shafiee, Indolinone-based acetylcholinesterase inhibitors: synthesis, biological activity and molecular modeling, *European Journal of Medicinal Chemistry* (2014), doi: 10.1016/j.ejmech.2014.01.017.

Graphical Abstract

Indolinone-based acetylcholinesterase inhibitors: synthesis, biological activity and molecular modeling

Hamidreza Akrami, Bibi Fatemeh Mirjalili, Mehdi Khoobi, Hamid Nadri, Alireza Moradi, Amirhossein Sakhteman, Saeed Emami, Alireza Foroumadi, Abbas Shafiee

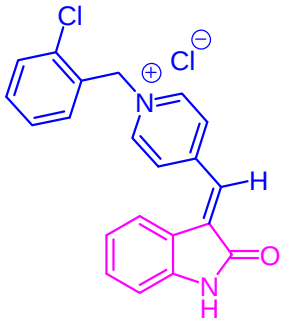

3c

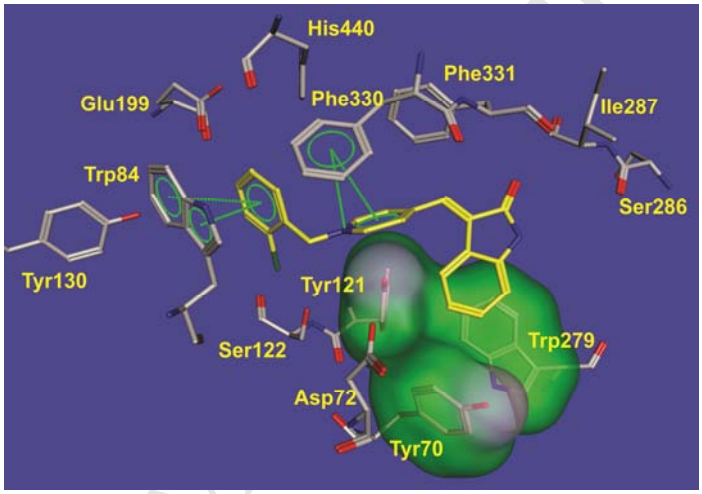

Indolinone-based compounds bearing benzylpyridinium moiety was designed as dual-binding inhibitors of AChE. 2-Chlorobenzyl derivative **3c** (IC_{50} = 0.44 nM) was 32-fold more potent than donepezil as reference drug.

Indolinone-based acetylcholinesterase inhibitors: synthesis, biological activity and molecular modeling

Hamidreza Akrami [a], Bibi Fatemeh Mirjalili [a], Mehdi Khoobi [b], Hamid Nadri [c], Alireza Moradi [c], Amirhossein Sakhteman [c], Saeed Emami [d], Alireza Foroumadi [b], Abbas Shafiee [b,*]

[a]*Department of Chemistry, College of Science, Yazd University, Yazd, PO Box 8915813149, Islamic Republic of Iran*

[b]*Department of Medicinal Chemistry, Faculty of Pharmacy and Pharmaceutical Sciences Research Center, Tehran University of Medical Sciences, Tehran 14176, Iran*

[c] *Department of Medicinal Chemistry, Faculty of Pharmacy, Shahid Sadoughi University of Medical Sciences-Yazd, Iran*

[d]*Department of Medicinal Chemistry and Pharmaceutical Sciences Research Center, Faculty of Pharmacy, Mazandaran University of Medical Sciences, Sari, Iran*

Abstract: A series of indolinone-based compounds bearing benzylpyridinium moiety was designed as dual-binding inhibitors of acetylcholinesterase (AChE). The target compounds **3a-u** were synthesized by condensation of oxindole and pyridin-4-carbalehyde, and subsequent *N*-benzylation. The anti-cholinesterase activity evaluation of synthesized compounds revealed that most of them had very potent inhibitory activity against AChE, superior to standard drug donepezil. Particularly, 2-chlorobenzyl derivative **3c** was the most potent compound against AChE with IC_{50} value of 0.44 nM, being 32-fold more potent than donepezil. Also, most of compounds were more potent than standard drug donepezil against butyrylcholinesterase (BuChE). Docking study revealed that the hydrophobic aromatic part (indoline) of representative compound **3c** binds to the PAS and the *N*-benzylpyridinium residue binds to the CAS of AChE.

Keywords: Alzheimer's disease, Acetylcholinesterase, Indolinone, Oxindole, Docking study

*Corresponding author. Tel: +98 21 66406757; Fax: +98 21 66461178.
E-mail address: ashafiee@ams.ac.ir (A. Shafiee).

1. Introduction

Alzheimer's disease (AD) is a neurodegenerative disorder characterized by a progressive decline in memory, learning and cognitive functions. Currently, it is estimated that AD affects about 36 million people worldwide and expecting to reach 66 million by 2030 [1]. AD is involved with a loss of presynaptic cholinergic function in the areas of the brain related to memory and learning. This neurological disorder is also associated with the presence of amyloid β-peptide (Aβ) deposits and neurofibrillary tangles in the brain [2]. The enhancement of cholinergic neurotransmission by preserving acetylcholine (ACh) levels would be an effective way to overcome the occurrence, symptoms and progression of AD [3,4]. Accordingly, the inhibition of acetylcholinesterase (AChE) which is responsible for the metabolic breakdown of ACh has been regarded as one of the most promising approaches [5]. Therefore, anti-AChE drugs such as donepezil, rivastigmine, galanthamine and tacrine, were developed for treatment of AD [6]. Among the anti-AChE drugs, tacrine is associated with hepatotoxicity thus it is rarely used [7]. On the other hand, donepezil and rivastigmine which are commonly used in the early-to-moderate stages of AD often present adverse effects and are not completely effective [8]. However, clinical trial studies revealed that galantamine shows promising pharmacological profile and clinically relevant neuroprotective effects in AD [9]. Therefore, design of more effective anti-AChE drugs with low side effects and better pharmacokinetics properties is an urgent need in the field of AD pharmacotherapy.

Previous studies on the structure and function of AChE revealed that this enzyme has two binding sites; catalytic anionic site (CAS) and peripheral anionic site (PAS) [10]. It was proposed that PAS could promote the deposition and aggregation of Aβ in the brain [11]. Accordingly, the multi-binding inhibitors which can inhibit catalytic activity of AChE and perturb the self-assembly of Aβ could be more effective agents for the management of AD [12]. For example, the dual-binding mode of donepezil with AChE has been demonstrated by

X-ray crystallography and docking studies. While the hydrophobic aromatic part (5,6-dimethoxyindan-1-one) of donepezil binds to the PAS, the *N*-benzyl piperidine residue binds to the CAS of AChE [13]. Accordingly, it was found that the presence of functionalized amine group such as benzyl piperidine, benzylamino, phenylpiperazine, and anilino moieties contribute to inhibitor activity by interacting with the catalytic site of the AChE. On the other hand, a ligand that is rich in aromatic groups, may engage to favorable stacking interactions with PAS [15]. Numbers of aromatic and heteroaromatic rings were found in AChE inhibitors as PAS binding scaffolds [16,17]. Recently, we introduced benzofuranone-based AChE-inhibitors containing benzylpyridinium moiety (Fig. 1) [18a]. In continuation of our previous efforts in order to find new AChE inhibitors [18], in this work we describe indolinone-based compounds bearing benzylpyridinium moiety as dual-binding inhibitors of AChE.

2. Results and discussion

2.1. Chemistry

The oxindole derivatives **3a-u** were synthesized via the route outlined in Scheme 1. In the first step, (*E*)-3-(pyridin-4-ylmethylene)indolin-2-one (**2**) were synthesized using oxindole (**1**) and pyridin-4-carbalehyde in the presence of *para*-toluene solfunic acid (PTSA) as a catalyst. Several acid catalysts and solvents were screened for this reaction but the best results were obtained in the presence of PTSA in refluxing toluene. In this reaction, the (*E*)-isomer was the major product which further crystallized from acetonitrile to obtain the pure (*E*)-**2**. The chemical shift of the vinylic proton could be used to assign the configuration of product. In the (*E*)-geometry of compound **2**, the vinylic proton would be shifted downfield due to deshielding effect of carbonyl group [19]. According to the literature reports, the vinylic hydrogen in (*E*)-isomers is appeared at 7.6–8.0 ppm [20]. The target compounds **3a-u** were easily prepared by the reaction of proper benzyl bromide or chloride with compound

(*E*)-**2**. Accordingly, the reaction mixture was stirred in dry acetonitirile without catalyst, at 60–70 ºC for 6–24 h. On cooling, the product was precipitated as a solid which was separated, washed with diethyl ether or *n*-hexane and recrystallized from ethanol-water. The ^{1}H NMR data of final compounds **3** revealed that the (*E*)-geometry of compounds have been preserved based on the downfield chemical shifts of vinilic proton ($\delta > 7.9$ ppm).

2.2. Inhibitory activity against AChE and BuChE

The IC_{50} values of test compounds against AChE reveled that compounds **3b**, **3c**, **3e**, **3g**, **3i-m** showed very potent inhibitory activity (IC_{50} values = 0.44–12.8 nM) superior to standard drug donepezil. Among them, 2-chlorobenzyl derivative **3c** was the most potent compound against AChE, with IC_{50} value of 0.44 nM. This compounds was about 32-fold more potent than donepezil. Moreover, 2-fluoro and 2-bromo analogues (compounds **3b** and **3e**, respectively) with IC_{50} values ≤1.46 nM showed high activity against AChE. The comparison of un-substituted compound **3a** with *ortho*- or *meta*-substituted analogues **3b-m** demonstrated that introduction of halo, methyl and methoxy group at 2- or 3-position of *N*-benzyl pendent residue significantly improved the anti-AChE activity. The 2-chloro substituent had the most impact on the AChE inhibition of designed compounds. In contrast, introduction of different substituents on the *para*-position of benzyl group diminished the inhibitory activity against AChE (**3n-r** vs. **3a**). As shown by compound **3r**, the 4-nitro group more significantly decreased the activity. Interestingly, the insertion of second chlorine atom on *ortho* or *meta* positions of 4-chlorobenzyl derivative **3o** resulted in more potent compounds **3s** and **3t**. While, in the case of 2- or 3-chlorobenzyl derivatives (compounds **3c** or **3i**, respectively), introduction of second halogen decreased the anti-AChE activity as observed with compounds **3g**, **3h**, **3s** and **3t**. The displacement of halogen atom (Br, Cl and

F) on benzyl group dramatically affects the anti-AChE activity. The order of activity was as follow: 2-halo > 3-halo > 4-halo.

The observed IC_{50} values of target compounds against BuChE revealed that all compounds with the exception of **3q** and **3r** were more potent than standard drug donepezil. The anti-BuChE activity of the most potent compound **3d** was 6 times higher than that of donepezil. Most of substituted benzyl compounds were more potent than unsubstituted analogue **3a** against BuChE. These results showed that substitution on benzyl group had often positive effect on anti-BuChE avtivity. The highest activity was observed with 2-methyl analogue. However, 3-fluoro, 4-methoxy and 4-nitro substituents decreased the inhibitory activity against BuChE.

As calculated in Table 1, the most active compound against AChE (compound **3c**) showed very high selectivity for this enzyme (SI = 3113). Moreover, other potent compounds **3b** and **3e** had high selectivity for AChE (SI > 842).

2.3. Docking studies

In order to gain functional and structural insight into the binding mode of the compounds, molecular docking simulation was performed using Autodock Vina software. To confirm the validity of used docking parameters, the co-crystallized ligand E2020 was re-docked into the active site of AChE and the RMSD value (0.87 Å) guaranteed the validity of the docking procedure (Fig. 2). Subsequently, the most active compound **3c** was docked using the optimized parameters. Regarding the docking studies, three types of interactions; hydrophobic interaction, hydrophobic π-π interaction and π-cation interaction were involved in the attachment of ligand to the active site of the enzyme. The quaternary nitrogen of the pyridinium ring facilitates ligand recognition through binding to mid-gorge recognition site comprising Phe330. The ligand is anchored at the bottom of active site through a π-cation

interaction with Phe330 along with a π-π interaction with Trp84 in the catalytic anionic site (CAS). In addition, the indole moiety was well fitted in the hydrophobic pocket composed by Tyr70, Tyr121 and Trp279 in the peripheral anionic site (PAS) (Fig. 3). These key interactions are similar to those of well-known AChE inhibitors complexed with the enzyme.

To get better insight to the concluded SAR, the best pose of both more and less active compounds (**3c** and **3r**, respectively) were also overlaid and shown in Fig. 4. As illustrated in Figure 4, the binding modes are similar in a way that two π-π interactions were observed with Trp84 and Phe330. However, substitution on the *para* position of compound **3r** was not tolerated due to the steric hindrance with the residues in the bottom of active site (CS). To get rid of the steric hindrance, the orientation of (4-nitrobenzyl)pyridinium fragment of compound **3r** was changed, leading to weak π-π interactions. These finding could explain the lower potency of 4-substituted benzylpyridinium compounds.

2.4. Kinetics study

To gain further insight to the mechanism of action of these series of compounds on AChE, a kinetics study was performed on the most active compound **3c**. Graphical analysis of reciprocal Lineweaver–Burk plot revealed that this compound has shown mixed-type inhibition on AChE (Fig. 5). The type of inhibition is in agreement with the proposed binding mode of these compounds in the active-site gorge of AChE. Plotting of the slopes versus concentration of **3c** gave an estimation of inhibition constant, *K*i of 1.14 nM (Fig. 6).

2.5. ADMET prediction

The ADMET (absorption, distribution, metabolism, excretion and toxicity) properties of the target compounds were predicted using admetSAR web-based application [21]. The predicted ADMET data were included in the Supplementary Material. Based on the predicted values

for BBB penetration, all compounds might be able to pass through blood brain barrier and penetrate into the CNS and therefore, are considered as CNS active compounds. Moreover, all the compounds may not show either acute toxicity according to the calculated LC_{50} values nor mutagenic effect with respect to the AMES test data.

3. Conclusion

In conclusion, we have described indolinone-based compounds bearing benzylpyridinium moiety as dual-binding inhibitors of AChE. The target compounds **3a-u** were synthesized by condensation of oxindole (**1**) and pyridin-4-carbalehyde to obtain (*E*)-3-(pyridin-4-ylmethylene)indolin-2-one (**2**), and subsequent *N*-benzylation with benzyl halides. The anti-cholinesterase activity evalauation of synthesized compounds revealed that most of them had very potent inhibitory activity against AChE, superior to standard drug donepezil. Particularly, 2-chlorobenzyl derivative **3c** was the most potent compound against AChE, with IC_{50} value of 0.44 nM. This compounds was about 32-fold more potent than donepezil. Also, all compounds with the exception of **3q** and **3r** were more potent than standard drug donepezil against BuChE. Docking study revealed that the hydrophobic aromatic part (indoline) of representative compound **3c** binds to the PAS and the *N*-benzylpyridinium residue binds to the CAS of AChE. Kinetics study with compound **3c** demonstrated that this compound has mixed-type inhibition on AChE. The favorable *in silico* ADMET properties of designed compounds with *in vitro* anti-cholinesterase potential of compounds make them as new lead compounds for further optimization in the field of AD pharmacotherapy.

4. Experimental protocols

4.1. Chemistry

All commercially available reagents were purchased from Merck AG or Aldrich and used without further purification. Melting points were measured on the Buchi Melting point B-540. FT-IR spectra were run on a Bruker, Eqinox 55 spectrometer (KBr disks). Mass spectra of the products were obtained with an HP (Agilent technologies) 5937 Mass Selective Detector. ^{1}H NMR spectra were recorded on a Bruker 500 MHz NMR instrument. Elemental analyses were carried out by a CHN-Rapid Heraeus elemental analyzer. The results of elemental analyses (C, H, N) were within ±0.4% of the calculated values.

*4.1.1. Synthesis of (E)-3-(pyridin-4-ylmethylene)indolin-2-one (**2**)*

A mixture of oxindole (**1**, 1 mmol), pyridine-4-carbaldehyde (1 mmol), and PTSA (1 mmol) was refluxed in dry toluene for 3 h. After completion of the reaction (monitored by TLC), the solvent was evaporated under vacuum. Then, sodium carbonate solution 30% (15 mL) was added and extracted with chloroform (3×15 mL). The organic phase was dried (Na_2SO_4) and the solvent was evaporated under vacuum to obtain yellow solid. The solid was recrystallized from acetonitrile to afford pure product **2**. Yellow solid; yield 78%; mp 182-184 ºC; IR (KBr, cm^{-1}): 3417, 1712, 1615, 1597; ^{1}H NMR (500 MHz, DMSO-d_6) δ: 8.76 (d, *J* = 5.9 Hz, 2H, H-a), 8.45 (s, 1H, NH), 7.70 (s, 1H, H-vinylic), 7.52 (d, *J* = 5.8 Hz, 2H, H-b), 7.46 (d, *J* = 7.7 Hz, 1H, H-4), 7.28-7.25 (m, 1H, H-6), 6.91 (d, *J* = 7.7 Hz, 1H, H-7), 6.91-6.87 (m, 1H, H-5). Anal. Calcd for $C_{14}H_{10}N_2O$ (222.24): C, 75.66; H, 4.54; N, 12.60. Found: C, 75.31; H, 4.74; N, 12.39.

*4.1.2. General procedure for the preparation of compounds **3a-u***

To a mixture of (*E*)-3-(pyridin-4-ylmethylene)indolin-2-one (**2**, 1 mmol) in dry acetonitrile (5 mL), proper benzyl bromide or chloride (1.5 mmol) was added and the mixture was stirred at 60-70 ºC for 6-24 h. Then, the mixture was cooled and the precipitated solid was filtrated off

and washed with diethyl ether or *n*-hexane. The product was recrystallized from ethanol-water (1:1) to give pure compounds **3a-u**.

*4.1.2.1. (E)-1-(benzyl)-4-((2-oxoindolin-3-ylidene)methyl)pyridinium bromide (**3a**)*

Red solid; yield 92%; mp 224-226 ºC; IR (KBr, cm^{-1}): 3430, 1696, 1634; ^{1}H NMR (500 MHz, DMSO-d_6) δ: 10.97 (s, 1H, NH), 9.27 (d, *J* = 5.3 Hz, 2H, H-a), 8.73 (d, *J* = 5.4 Hz, 2H, H-b), 7.99 (s, 1H, H-vinylic), 7.77 (d, *J* = 7.2 Hz, 1H, H-4), 7.60-7.45 (m, Ar $H_{2,3,4,5}$), 7.32 (t, *J* = 7.3 Hz, 1H, H-6), 7.05 (t, *J* = 7.4, 1H, H-5), 6.87 (d, *J* = 7.4 Hz, 1H, H-7), 5.88 (s, 2H, $-CH_2N^+$). ^{13}C NMR (DMSO-d_6, 125 MHz) δ: 166.3, 149.4, 144.1, 142.7, 135.4, 134.3, 131.9, 129.3, 129.2, 128.7, 128.6, 128.2, 123.1, 121.8, 121.7, 110.2, 62.8. MS m/z (%) 313 (M^+, 4), 222 (100), 194 (29), 166 (15), 144 (74), 91 (97), 65 (16), 51 (14). Anal. Calcd for $C_{21}H_{17}BrN_2O$ (393.28): C, 64.13; H, 4.36; N, 7.12. Found: C, 64.50; H, 4.15; N, 7.37.

*4.1.2.2. (E)-1-(2-fluorobenzyl)-4-((2-oxoindolin-3-ylidene)methyl)pyridinium chloride (**3b**)*

Red solid; yield 91%; mp 234-236 ºC; IR (KBr, cm^{-1}): 3191, 1696, 1643; ^{1}H NMR (500 MHz, DMSO-d_6) δ: 10.92 (s, 1H, NH), 9.15 (br s, 2H, H-a), 8.73 (br s, 2H, H-b), 7.97 (s, 1H, H-vinylic), 7.77 (br s, 1H, H-4), 7.64 (br s, 1H, Ar H_6), 7.54 (br s, 1H, Ar H_4), 7.34 (br s, 3H, Ar $H_{3,5}$, H-6), 7.06 (br s, 1H, H-5), 6.88 (br s, 1H, H-7), 6.02 (s, 2H, $-CH_2N^+$). ^{13}C NMR (DMSO-d_6, 125 MHz) δ: 166.3, 149.8, 144.3, 142.7, 135.5, 132.1, 132.09, 132.02, 131.5, 128.7, 128.4, 125.3, 123.1, 121.9, 121.8, 121.2, 121.1, 116.1, 115.9, 110.2, 57.5. Anal. Calcd for $C_{21}H_{16}ClFN_2O$ (366.82): C, 68.76; H, 4.40; N, 7.64. Found: C, 68.52; H, 4.12; N, 7.95.

*4.1.2.3. (E)-1-(2-chlorobenzyl)-4-((2-oxoindolin-3-ylidene)methyl)pyridinium chloride (**3c**)*

Red solid; yield 90%; mp 225-227 ºC; IR (KBr, cm^{-1}): 3396, 1690, 1632; ^{1}H NMR (500 MHz, DMSO-d_6) δ: 10.95 (s, 1H, NH), 9.12 (d, *J* = 6.8 Hz, 2H, H-a), 8.75 (d, *J* = 6.8 Hz, 2H,

H-b), 8.00 (s, 1H, H-vinylic), 7.78 (d, *J* = 7.5 Hz, 1H, H-4), 7.61 (d, *J* =7.7 Hz, 1H, Ar H_3), 7.54-7.48 (m, 3H, Ar $H_{4,5,6}$), 7.35 (t, *J* = 7.5 Hz, 1H, H-6), 7.06 (t, *J* = 7.5 Hz, 1H, H-5), 6.88 (d, *J* = 7.5 Hz, 1H, H-7), 5.99 (s, 2H, $-CH_2N^+$). ^{13}C NMR (DMSO-d_6, 125 MHz) δ: 166.3, 149.9, 144.5, 142.8, 135.6, 133.3, 132.0, 131.6, 131.4, 131.3 130.1, 128.6, 128.4, 128.1, 123.2, 121.9, 121.8, 110.2, 60.8. Anal. Calcd for $C_{21}H_{16}Cl_2N_2O$ (383.27): C, 65.81; H, 4.21; N, 7.38. Found: C, 65.60; H, 4.43; N, 7.70.

*4.1.2.4. (E)-1-(2-methylbenzyl)-4-((2-oxoindolin-3-ylidene)methyl)pyridinium chloride (**3d**)*

Red solid; yield 88%; mp 214-217 ºC; IR (KBr, cm^{-1}): 3418, 1700, 1634; ^1H NMR (500 MHz, DMSO-d_6) δ: 11.00 (s, 1H, NH), 9.09. (d, *J* = 5.5 Hz, 2H, H-a), 8.74 (d, *J* = 5.5 Hz, 2H, H-b), 8.02 (s, 1H, H-vinylic), 7.78 (d, *J* = 7.2 Hz, 1H, H-4), 7.32-7.28 (m, 4H, Ar $H_{3,4,5,6}$), 7.20 (t, *J* = 7.2 Hz, 1H, H-6), 7.04 (t, *J* = 7.2 Hz, 1H, H-5), 6.87 (d, *J* = 7.2, 1H, H-7), 5.93 (s, 2H, $-CH_2N^+$), 2.32 (s, 3H, $-CH_3$). ^{13}C NMR (DMSO-d_6, 125 MHz) δ: 166.3, 149.6, 144.3, 142.7, 135.4, 132.3, 131.9, 130.9, 129.3, 129.2, 128.6, 127.8, 126.7, 123.2, 121.9, 121.8, 110.2, 61.0, 18.8. MS m/z (%) 327 (M^+, 4), 222 (94), 194 (28), 144 (62), 139 (60), 105 (100), 77 (26), 51 (28). Anal. Calcd for $C_{22}H_{19}ClN_2O$ (362.85): C, 72.82; H, 5.28; N, 7.72. Found: C, 72.60; H, 5.55; N, 72.91.

4.1.2.5. (E)-1-(2-bromobenzyl)-4-((2-oxoindolin-3-ylidene)methyl)pyridinium chloride (***3e***)

Red solid; yield 91%; mp 150-152 ºC; IR (KBr, cm^{-1}): 3406, 1702, 1633; ^1H NMR (500 MHz, DMSO-d_6) δ: 10.95 (s, 1H, NH), 9.10 (d, *J* = 6.2 Hz, 2H, H-a), 8.76 (d, *J* = 6.2 Hz, 2H, H-b), 8.01 (s, 1H, H-vinylic), 7.78-7.75 (m, 2H, Ar H_3, H-4), 7.53 (t, *J* = 7.2 Hz, 1H, Ar H_5), 7.46-7.43 (m, 2H, Ar $H_{4,6}$), 7.34 (t, *J* = 7.5 Hz, 1H, H-6), 7.06 (t, *J* = 7.5 Hz, 1H, H-5), 6.88 (d, *J* = 7.5 Hz, 1H, H-7), 5.97 (s, 2H, $-CH_2N^+$). ^{13}C NMR (DMSO-d_6, 125 MHz) δ: 166.3, 149.9, 144.6, 142.8, 137.0, 135.6, 133.4, 133.03, 132.07, 131.5, 128.7, 128.6, 128.5, 123.5,

123.2, 121.9, 121.8, 110.2, 62.9. Anal. Calcd for $C_{21}H_{16}BrClN_2O$ (427.72): C, 58.97; H, 3.77; N, 6.55. Found: C, 58.66; H, 4.11; N, 6.80.

*4.1.2.6. (E)-1-(2-nitrobenzyl)-4-((2-oxoindolin-3-ylidene)methyl)pyridinium bromide (**3f**)*

Red solid; yield 89%; mp 271-273 ºC; IR (KBr, cm^{-1}): 3404, 1707, 1634, 1525, 1343; ^1H NMR (500 MHz, DMSO-d_6) δ: 10.93 (s, 1H, NH), 9.08. (d, *J* = 6.3 Hz, 2H, H-a), 8.78 (d, *J* = 6.3 Hz, 2H, H-b), 8.29 (s, 1H, H-vinylic), 7.88-7.85 (m, 2H, Ar H_3, H-4), 7.79 (br s, 2H, Ar $H_{3,5}$), 7.36-7.31 (m, 3H, Ar $H_{4,6}$, H-6), 7.07 (t, *J* = 7.8 Hz, 1H, H-5), 6.89 (d, *J* = 7.8 Hz, 1H, H-7), 6.21 (s, 2H, $-CH_2N^+$). Anal. Calcd for $C_{21}H_{16}BrN_3O_3$ (438.27): C, 57.55; H, 3.68; N, 9.59. Found: C, 57.32; H, 3.32; N, 9.80.

*4.1.2.7. (E)-1-(2-chloro-6-fluorobenzyl)-4-((2-oxoindolin-3-ylidene)methyl)pyridinium chloride (**3g**)*

Red solid; yield 92%; mp 261-263 ºC; IR (KBr, cm^{-1}): 3360, 1695, 1632; ^1H NMR (500 MHz, DMSO-d_6) δ: 10.97 (s, 1H, NH), 9.05 (d, *J* = 5.7 Hz, 2H, H-a), 8.72 (d, *J* = 5.7 Hz, 2H, H-b), 8.00 (s, 1H, H-vinylic), 7.76 (d, *J* = 7.5 Hz, 1H, H-4), 7.3-7.61 (m, *J* = 7 Hz, 1H, Ar H_5), 7.51 (d, *J* = 7.9, 1H, Ar H_3), 7.44 (t, *J* = 7.9 Hz, 1H, Ar H_4), 7.33 (t, *J* = 7.5 Hz, 1H, H-6), 7.04 (t, *J* = 7.5 Hz, 1H, H-5), 6.88 (d, *J* = 7.5 Hz, 1H, H-7), 6.04 (s, 2H, $-CH_2N^+$). MS m/z (%) 368 (M^++2, 4), 366 (M^+, 11), 222 (100), 221 (48), 194 (29), 143 (84), 144 (62), 107 (24), 89 (12), 51 (12). Anal. Calcd for $C_{21}H_{15}Cl_2FN_2O$ (401.26): C, 62.86; H, 3.77; N, 6.98. Found: C, 62.58; H, 3.97; N, 7.26.

*4.1.2.8. (E)-1-(2,6-dichlorobenzyl)-4-((2-oxoindolin-3-ylidene)methyl)pyridinium chloride (**3h**)*

Red solid; yield 89%; mp 187-189 ºC; IR (KBr, cm^{-1}): 3372, 1686, 1631; ^1H NMR (500 MHz, DMSO-d_6) δ: 10.92 (s, 1H, NH), 9.00 (d, *J* = 5.9 Hz, 2H, H-a), 8.72 (d, *J* = 5.9 Hz, 2H, H-b), 7.98 (s, 1H, H-vinylic), 7.77 (d, *J* = 7.7 Hz, 1H, H-4), 7.70 (d, *J* = 7.3 Hz, 2H, Ar $H_{3,5}$), 7.66-7.63 (m, 1H, Ar H_4), 7.39-7.35 (m, 1H, H-6), 7.06 (t, *J* = 7.7 Hz, 1H, H-5), 6.84 (d, *J* = 7.7 Hz, 1H, H-7), 6.13 (s, 2H, -CH_2N^+). Anal. Calcd for $C_{21}H_{15}Cl_3N_2O$ (417.72): C, 60.38; H, 3.62; N, 6.71. Found: C, 60.62; H, 3.85; N, 6.35.

*4.1.2.9. (E)-1-(3-chlorobenzyl)-4-((2-oxoindolin-3-ylidene)methyl)pyridinium bromide (**3i**)*

Red solid; yield 91%; mp 225-227 ºC; IR (KBr, cm^{-1}): 3175, 1695, 1633; ^1H NMR (500 MHz, DMSO-d_6) δ: 10.87 (s, 1H, NH), 9.20 (d, *J* = 6.6 Hz, 2H, H-a), 8.72 (d, *J* = 6.6 Hz, 2H, H-b), 7.95 (s, 1H, H-vinylic), 7.75 (d, *J* = 7.5 Hz, 1H, H-4), 7.73 (s, 1H, Ar H_2), 7.55-7.48 (m, 3H, Ar $H_{4,5,6}$), 7.33 (t, *J* = 7.5 Hz, 1H, H-6), 7.05 (t, *J* = 7.5 Hz, 1H, H-5), 6.85 (d, *J* = 7.5 Hz, 1H, H-7), 5.84 (s, 2H, -CH_2N^+). ^{13}C NMR (DMSO-d_6, 125 MHz) δ: 166.3, 149.7, 144.2, 142.7, 136.3, 135.4, 133.6, 132.03, 131.1, 129.3, 128.9, 128.7, 128.5, 127.6, 123.1, 121.9, 121.8, 110.1, 62.04. MS m/z (%) 349 (M^++2, 6), 347 (M^+, 17), 222 (100), 194 (27), 166 (20), 144 (60), 125 (90), 89 (40), 51 (20). Anal. Calcd for $C_{21}H_{16}BrClN_2O$ (427.72): C, 58.97; H, 3.77; N, 6.55. Found: C, 58.75; H, 3.95; N, 6.85.

*4.1.2.10. (E)-1-(3-bromobenzyl)-4-((2-oxoindolin-3-ylidene)methyl)pyridinium chloride (**3j**)*

Red solid; yield 86%; mp 183-185 ºC; IR (KBr, cm^{-1}): 3395, 1702, 1633; ^1H NMR (500 MHz, DMSO-d_6) δ: 10.97 (s, 1H, NH), 9.27 (d, *J* = 6.5 Hz, 2H, H-a), 8.73 (d, *J* = 6.5 Hz, 2H, H-b), 7.98 (s, 1H, H-vinylic), 7.90 (s, 1H, Ar H_2), 7.76 (d, *J* = 7.5 Hz, 1H, H-4), 7.64-7.60 (m, 2H, Ar $H_{4,6}$), 7.40 (t, *J* = 7.5 Hz, 1H, Ar H_5), 7.32 (t, *J* = 7.5 Hz, 1H, H-6), 7.03 (t, *J* = 7.5 Hz, 1H, H-5), 6.86 (d, *J* = 7.5 Hz, 1H, H-7), 5.87 (s, 2H, -CH_2N^+). Anal. Calcd for $C_{21}H_{16}BrClN_2O$ (427.72): C, 58.97; H, 3.77; N, 6.55. Found: C, 58.60; H, 3.54; N, 6.86.

*4.1.2.11. (E)-1-(3-methylbenzyl)-4-((2-oxoindolin-3-ylidene)methyl)pyridinium chloride (**3k**)*

Red solid; yield 85%; mp 225-227 ºC; IR (KBr, cm^{-1}): 3419, 1706, 1633; ^{1}H NMR (500 MHz, DMSO-d_6) δ: 10.94 (s, 1H, NH), 9.22 (d, *J* = 6.5 Hz, 2H, H-a), 8.71 (d, *J* = 6.5 Hz, 2H, H-b), 7.97 (s, 1H, H-vinylic), 7.75 (d, *J* = 5.5 Hz, 1H, H-4), 7.39 (s, 1H, Ar H_2), 7.35-7.32 (m, 3H, Ar $H_{4,5,6}$), 7.24 (br s, 1H, H-6), 7.03 (t, *J* = 5.5 Hz, 1H, H-5), 6.86 (d, *J* = 5.5 Hz, 1H, H-7), 5.80 (s, 2H, -CH_2N^+), 2.31 (s, 3H, -CH_3). ^{13}C NMR (DMSO-d_6, 125 MHz) δ: 166.3, 149.5, 144.09, 142.7, 138.6, 135.3, 134.2, 131.9, 129.3, 129.1, 128.7, 128.5, 127.8, 125.9, 123.1, 121.88, 121.81, 110.2, 62.8, 20.8. Anal. Calcd for $C_{22}H_{19}ClN_2O$ (362.85): C, 72.82; H, 5.28; N, 7.72. Found: C, 73.02; H, 5.54; N, 7.89.

*4.1.2.12. (E)-1-(3-methoxylbenzyl)-4-((2-oxoindolin-3-ylidene)methyl)pyridinium chloride (**3l**)*

Red solid; yield 90%; mp 223-225 ºC; IR (KBr, cm^{-1}): 3417, 1709, 1633; ^{1}H NMR (500 MHz, DMSO-d_6) δ: 11.02 (s, 1H, NH), 9.31 (d, *J* = 5.3 Hz, 2H, H-a), 8.72 (d, *J* = 5.3 Hz, 2H, H-b), 8.01 (s, 1H, H-vinylic), 7.76 (d, *J* = 7.0 Hz, 1H , H-4), 7.60 (s, 1H, Ar H_2), 7.38-7.26 (m, 3H, Ar $H_{4,5,6}$), 7.16 (t, *J* = 7.0 Hz, 1H, H-6), 7.02-6.99 (m, 1H, H-5), 6.87 (d, *J* =7.0 Hz, 1H, H-7), 5.84 (s, 2H, -CH_2N^+), 3.76 (s, 3H, -OCH_3). ^{13}C NMR (DMSO-d_6, 125 MHz) δ: 166.2, 149.5, 144.1, 142.7, 135.6, 135.4, 133.4, 131.9, 130.4, 128.6, 128.4, 127.7, 123.7, 123.2, 121.9, 121.7, 121.4, 110.2, 62.6, 55.2. Anal. Calcd for $C_{22}H_{19}ClN_2O_2$ (378.85): C, 69.75; H, 5.05; N, 7.39. Found: C, 69.50; H, 5.27; N, 7.75.

*4.1.2.13. (E)-1-(3-fluorobenzyl)-4-((2-oxoindolin-3-ylidene)methyl)pyridinium chloride (**3m**)*

Red solid; yield 95%; mp 226-228 ºC; IR (KBr, cm^{-1}): 3428, 1695, 1633; ^{1}H NMR (500 MHz, DMSO-d_6) δ: 10.95 (s, 1H, NH), 9.28 (d, *J* = 6.8 Hz, 2H, H-a), 8.73 (d, *J* = 6.8 Hz, 2H,

H-b), 7.98 (s, 1H, H-vinylic), 7.76 (d, *J* = 6.9 Hz, 1H, H-4), 7.54-7.50 (m, 2H, Ar $H_{2,4}$), 7.46-7.44 (m, 1H, Ar H_6), 7.35-7.32 (m, 1H, Ar H_5), 7.28 (t, *J* = 6.9 Hz, 1H, H-6), 7.04 (t, *J* = 6.9 Hz, 1H, H-5), 6.86 (d, *J* = 6.9 Hz, 1H, H-7), 5.89 (s, 2H, -CH_2N^+). Anal. Calcd for $C_{21}H_{16}ClFN_2O$ (366.82): C, 68.76; H, 4.40; N, 7.64. Found: C, 68.52; H, 4.67; N, 7.35.

*4.1.2.14. (E)-1-(4-fluorobenzyl)-4-((2-oxoindolin-3-ylidene)methyl)pyridinium chloride (**3n**)*

Red solid; yield 94%; mp 140-142 ºC; IR (KBr, cm^{-1}): 3339, 1699, 1634; ^{1}H NMR (500 MHz, DMSO-d_6) δ: 10.90 (s, 1H, NH), 9.20 (d, *J* = 6.2 Hz, 2H, H-a), 8.72 (d, *J* = 6.2 Hz, 2H, H-b), 7.95 (s, 1H, H-vinylic), 7.75 (d, *J* = 7.0 Hz, 1H, H-4), 7.67 (br s, 2H, Ar $H_{3,5}$), 7.33 (br s, 3H, Ar $H_{2,6}$, H-6), 7.06 (br s, 1H, H-5), 6.86 (d, *J* = 7.0 Hz, 1H, H-7), 5.83 (s, 2H, -CH_2N^+). MS m/z (%) 331 (M^+, 20), 222 (100), 194 (29), 166 (18), 144 (83), 109 (100), 89 (20), 83 (22), 51 (24). Anal. Calcd for $C_{21}H_{16}ClFN_2O$ (366.82): C, 68.76; H, 4.40; N, 7.64. Found: C, 68.96; H, 4.62; N, 7.47.

*4.1.2.15. (E)-1-(4-chlorobenzyl)-4-((2-oxoindolin-3-ylidene)methyl)pyridinium chloride (**3o**)*

Red solid; yield 91%; mp 184-186 ºC; IR (KBr, cm^{-1}): 3389, 1699, 1632; ^{1}H NMR (500 MHz, DMSO-d_6) δ: 10.91 (s, 1H, NH), 9.19 (d, *J* = 6.3 Hz, 2H, H-a), 8.72 (d, *J* = 6.3 Hz, 2H, H-b), 7.96 (s, 1H, H-vinylic), 7.76 (d, *J* = 7.6 Hz, 1H , H-4), 7.61 (d, *J* = 8.5 Hz, 2H, Ar $H_{2,6}$), 7.55 (d, *J* = 8.5 Hz, 2H, Ar $H_{3,5}$), 7.32-7.35 (m, 1H, H-6), 7.06 (t, *J* = 7.6 Hz, 1H, H-5), 6.87 (d, *J* = 7.6 Hz, 1H, H-7), 5.84 (s, 2H, -CH_2N^+). Anal. Calcd for $C_{21}H_{16}Cl_2N_2O$ (383.27): C, 65.81; H, 4.21; N, 7.31 Found: C, 66.07; H, 4.48; N, 7.45.

*4.1.2.16. (E)-1-(4-bromobenzyl)-4-((2-oxoindolin-3-ylidene)methyl)pyridinium chloride (**3p**)*

Red solid; yield 90%; mp 148-150 ºC; IR (KBr, cm^{-1}): 3394, 1701, 1633; ^{1}H NMR (500 MHz, DMSO-d_6) δ: 10.93 (s, 1H, NH), 9.21 (d, *J* = 6.3 Hz, 2H, H-a), 8.72 (d, *J* = 6.3 Hz, 2H,

H-b), 7.97 (s, 1H, H-vinylic), 7.76 (d, *J* = 7.3 Hz, 1H, H-4), 7.68 (d, *J* = 7.8 Hz, 2H, Ar $H_{3,5}$), 7.54 (d, *J* = 7.8 Hz, 2H, Ar $H_{2,6}$), 7.33 (t, *J* = 7.3 Hz, 1H, H-6), 7.06 (t, *J* = 7.3 Hz, 1H, H-5), 6.87 (d, *J* = 7.3 Hz, 1H, H-7), 5.84 (s, 2H, $-CH_2N^+$). Anal. Calcd for $C_{21}H_{16}BrClN_2O$ (427.72): C, 58.97; H, 3.77; N, 6.55; Found: C, 59.25; H, 3.66; N, 6.80.

*4.1.2.17. (E)-1-(4-methoxybenzyl)-4-((2-oxoindolin-3-ylidene)methyl)pyridinium chloride (**3q**)*

Red solid; yield 91%; mp 103-105 ºC; IR (KBr, cm^{-1}): 3400, 1699, 1633; ^1H NMR (500 MHz, DMSO-d_6) δ: 11.00 (s, 1H, NH), 9.26 (d, *J* = 6.2 Hz, 2H, H-a), 8.71 (d, *J* = 6.2 Hz, 2H, H-b), 7.99 (s, 1H, H-vinylic), 7.76 (d, *J* = 7.8 Hz, 1H , H-4), 7.58 (d, *J* = 8.4 Hz, 2H, Ar $H_{2,6}$), 7.05-6.95 (m, 3H, H-6, Ar $H_{3,5}$), 6.91 (t, *J* = 7.8 Hz, 1H, H-5), 6.87 (d, *J* = 7.8 Hz, 1H, H-7), 5.80 (s, 2H, $-CH_2N^+$), 3.76 (s, 3H, $-OCH_3$). ^{13}C NMR (DMSO-d_6, 125 MHz) δ: 166.3, 149.4, 143.8, 142.7, 135.3, 131.9, 130.9, 130.7, 130.3, 128.6, 127.7, 126.2, 123.2, 121.9, 121.8, 110.2, 62.4, 55.2. Anal. Calcd for $C_{22}H_{19}ClN_2O_2$ (378.85): C, 69.75; H, 5.05; N, 7.39. Found: C, 69.95; H, 5.40; N, 7.05.

*4.1.2.18. (E)-1-(4-nitrobenzyl)-4-((2-oxoindolin-3-ylidene)methyl)pyridinium chloride (**3r**)*

Red solid; yield 89%; mp 150-152 ºC; IR (KBr, cm^{-1}): 3394, 1700, 1633; ^1H NMR (500 MHz, DMSO-d_6) δ: 10.93 (s, 1H, NH), 9.26 (d, *J* = 6.3 Hz, 2H, H-a), 8.77 (d, *J* = 6.3 Hz, 2H, H-b), 7.98 (s, 1H, H-vinylic), 7.72-7.83 (m, 4H, Ar $H_{2,3,5,6}$), 7.62 (d, *J* =7.5 Hz, 1H, H-4), 7.33 (br s, 1H, H-6), 7.04 (br s, 1H, H-5), 6.86 (d, *J* = 7.5 Hz, 1H, H-7), 6.03 (s, 2H, $-CH_2N^+$). Anal. Calcd for $C_{21}H_{16}ClN_3O_3$ (393.82): C, 64.05; H, 4.09; N, 10.67; Found: C, 64.31; H, 4.21; N, 10.39.

*4.1.2.19. (E)-1-(3,4-dichlorobenzyl)-4-((2-oxoindolin-3-ylidene)methyl)pyridinium chloride (**3s**)*

Red solid; yield 90%; mp 235-237 ºC; IR (KBr, cm^{-1}): 3387, 1711, 1634; ^1H NMR (500 MHz, DMSO-d_6) δ: 10.65 (s, 1H, NH), 8.70 (d, *J* = 5.4 Hz, 2H, H-a), 7.61 (d, *J* = 5.4 Hz, 2H, H-b), 7.54 (s, 2H, Ar H_2, H-vinylic), 7.34 (d, *J* = 7.7 Hz, 2H, Ar-$H_{5,6}$), 7.23-7.26 (m, 2H, H-4,6), 6.87 (d, *J* = 7.7 Hz, 1H, H-7), 6.82 (t, *J* = 7.7 Hz, 1H, H-5), 5.82 (s, 2H, -CH_2N^+). Anal. Calcd for $C_{21}H_{15}Cl_3N_2O$ (417.72): C, 60.38; H, 3.62; N, 6.71; Found: C, 60.18; H, 3.95; N, 6.49.

*4.1.2.20. (E)-1-(2,4-dichlorobenzyl)-4-((2-oxoindolin-3-ylidene)methyl)pyridinium chloride (**3t**)*

Red solid; yield 94%; mp 171-173 ºC; IR (KBr, cm^{-1}): 3421, 1701, 1633; ^1H NMR (500 MHz, DMSO-d_6) δ: 10.95 (s, 1H, NH), 9.10 (d, *J* = 5.2 Hz, 2H, H-a), 8.74 (d, *J* = 5.2 Hz, 2H, H-b), 7.99 (s, 1H, H-vinylic), 7.81-7.78 (m, 2H, H-4, Ar H_3), 7.63-7.59 (m, 2H, Ar $H_{5,6}$), 7.32-7.35 (m, 1H, H-6), 7.05 (t, *J* = 6.8 Hz, 1H, H-5), 6.87 (d, *J* = 6.8, 1H, H-7), 5.97 (s, 2H, -CH_2N^+). MS m/z (%) 385 (M^++4, 3), 383 (M^++2, 19), 381 (M^+, 30), 222 (100), 194 (56), 166 (24), 159 (95), 144 (75), 89 (38), 63 (34), 51 (30). Anal. Calcd for $C_{21}H_{15}Cl_3N_2O$ (417.72): C, 60.38; H, 3.62; N, 6.71; Found: C, 60.18; H, 3.45; N, 6.91.

*4.1.2.21. (E)-1-(4-chloromethylbenzyl)-4-((2-oxoindolin-3-ylidene)methyl)pyridinium chloride (**3u**)*

Red solid; yield 92%; mp 121-123 ºC; IR (KBr, cm^{-1}): 3371, 1699, 1632; ^1H NMR (500 MHz, DMSO-d_6) δ: 10.95 (s, 1H, NH), 9.22 (d, *J* = 6.3 Hz, 2H, H-a), 8.69 (d, *J* = 6.3 Hz, 2H, H-b), 7.96 (s, 1H, H-vinylic), 7.75 (d, *J* = 7.5 Hz, 1H, H-4), 7.56 (d, *J* = 8.5 Hz, 2H, Ar $H_{3,5}$), 7.32 (t, *J* = 7.5 Hz, 1H, H-6), 7.04-6.99 (m, 3H, H-5, Ar $H_{2,6}$), 6.85 (d, *J* = 7.5 Hz, 1H, H-7),

5.77 (s, 2H, -CH_2N^+), 3.75 (s, 2H, -CH_2Cl). ^{13}C NMR (DMSO-d_6, 125 MHz) δ: 166.3, 159.9, 149.4, 143.8, 142.7, 135.2, 131.9, 130.7, 128.6, 128.5, 126.1, 123.1, 121.8, 121.7, 114.5, 110.1, 62.4, 55.2. Anal. Calcd for $C_{22}H_{18}Cl_2N_2O$ (397.30): C, 66.51; H, 4.57; N, 7.05. Found: C, 66.80; H, 4.25; N, 7.34.

4.2. In vitro inhibition studies on AChE and BuChE

The spectrophotometric method of Ellman [22] was used to assess the inhibitory activity of the target compounds toward AChE and BuChE. Acetylcholinesterase (AChE, E.C. 3.1.1.7, Type V-S, lyophilized powder, from *electric eel*, 1000 unit), butyrylcholinesterase (BuChE, E.C. 3.1.1.8, from equine serum), and butyrylthiocholine iodide (BTC) were purchased from Sigma–Aldrich. 5,5′-Dithiobis-(2-nitrobenzoic acid) (DTNB), potassium dihydrogen phosphate, dipotassium hydrogen phosphate, potassium hydroxide, sodium hydrogen carbonate, and acetylthiocholine iodide were obtained from Fluka. The reaction took place in a final mixture of 3 mL phosphate buffer (0.1M, pH = 8.0), 100 µL of DTNB solution, 100 µL of 2.5 unit/mL enzyme solution (AChE) and 100 µL of each tested compounds. The above mixture was pre-incubated for 10 min prior to adding 20 µL of substrate (acetylthiocholine iodide). Changes in absorbance were detected at 412 nm for 6 minutes and the IC_{50} values were determined graphically from inhibition curves. Five different concentrations for each compound were tested to obtain the range of 20% to 80% enzyme inhibition. All experiments were performed in triplicate at 25°C on a UV Unico Double Beam Spectrophotometer. The same method was also taken for BuChE inhibition assay.

4.3. Kinetics study

To obtain estimates of the inhibition constant K_i and inhibition model of compounds, reciprocal plots of 1/v versus 1/[s] were constructed at different concentrations of the

substrate acetylthiocholine (0.14-0.69 mM) by using Ellman's method. The experiments were performed as same as enzyme inhibition assay in triplicate. The rate of enzyme activity was measured in the presence of different concentrations of inhibitor and without inhibitor for proposed concentrations of substrate. For each experiment after adding acetylthiocholine as substrate, progress curves were monitored at 420 nm for 2 min. Then the double reciprocal plots (1/v vs. 1/[s]) were constructed using the slopes of progress curves to obtain the type of inhibition. Slopes of the reciprocal plots were then plotted against the concentration of inhibitor, to evaluate K_i data. Data analysis was performed with Microsoft Excel 2003.

4.4. Molecular modeling

The crystal structure of acetylcholinesterase complexed with E2020 (code ID: 1EVE) was obtained from the Protein Data Bank. Then, the water molecules and inhibitor were removed. Further preparation of protein was performed by Autodock Tools (ver 1.5.4) [23] using default parameters and finally saved as pdbqt format. The 2D structures of ligands were generated using MarvineSketch 5.8.3, 2012, ChemAxon (http://www.chemaxon.com) and then converted to 3D and pdbqt format by Openbabel (ver. 2.3.1) [24]. Docking studies were carried out using the Autodock Vina (ver. 1.1.1) program [25]. The search space was defined as a box with following parameters: size_x=40, size_y=40, size_z=40 which centered on the geometrical center of co-crystallized ligand using these parameters: center_x=2.023, center_y=63.295, center_z=67.062. The exhaustiveness was set to 80 and other parameters were left as default values. Finally, the most favorable conformations based on the free energy of binding were selected for analyzing the interactions between the AChE and inhibitor. All the 3D models are depicted using the Chimera 1.6 software [26].

Acknowledgments

This research was supported by grants from the research council of Tehran University of Medical Sciences and the Iran National Science Foundation (INSF). Molecular graphics and analyses were performed with the UCSF Chimera package. Chimera is developed by the 25 Resource for Biocomputing, Visualization, and Informatics at the University of California, San Francisco.

References

[1] Alzheimer's Disease International, World Alzheimer Report, 2011, p. 1.

[2] C. Ballard, S. Gauthier, A. Corbett, C. Brayne, D. Aarsland, E. Jones, Lancet 377 (2011) 1019–1031.

[3] M. Weinstock, J. Neural Transm. 49 (1997) 93–102.

[4] C.G. Ballard, N.H. Greig, A.L. Guillozet-Bongaarts, A. Enz, S. Darvesh, Curr. Alzheimer Res. 2 (2005) 307–318.

[5] E. Scarpini, P. Scheltens, H. Feldman, Lancet Neurol. 2 (2003) 539–547.

[6] B.M. McGleenon, K.B. Dynan, A.P. Passmore, Br. J. Clin. Pharmacol. 48 (1999) 471–480.

[7] A. Lleo, S.M. Greenberg, J.H. Growdon, Annu. Rev. Med. 57 (2006) 513–533.

[8] L.L. Shen, G.X. Liu, Y. Tang, Acta. Pharmacol. Sin 28 (2007) 2053–2063.

[9] J. Marco-Contelles, M.D. Carreiras, C. Rodriguez, M. Villarroya, A.G. Garcia, Chem. Rev. 106 (2006) 116–133.

[10] J.L. Sussman, M. Harel, F. Frolow, C. Oefner, A. Goldman, L. Toker, I. Silman, Science 253 (1991) 872–879.

[11] M. Pera, A. Martinez-Otero, L. Colombo, M. Salmona, D. Ruiz-Molina, A. Badia, et al., Mol. Cell Neurosci. 40 (2009) 217–24.

[12] E. Giacobini, Neurochem. Res. 28 (2003) 515–22.

[13] G. Koellner, G. Kryger, C.B. Millard, I. Silman, J.L. Sussman, T. Steiner, J. Mol. Biol. 296 (2000) 713–735.

[14] A. Saxena, J.M. Fedorko, C.R. Vinayaka, R. Medhekar, Z. Radić, P. Taylor, O. Lockridge, B.P. Doctor, Eur. J. Biochem. 270 (2003) 4447–4458.

[15] R. León, A.G. Garcia, J. Marco-Contelles, Med. Res. Rev. 33 (2013) 139–189.

[16] W. Tong, E.R. Collantes, Y. Chen, W.J. Welsh, J. Med. Chem. 39 (1996) 380–387.

[17] J.Q. Araújo, M.A. de Brito, L.V. Hoelz, R.B. de Alencastro, H.C. Castro, C.R. Rodrigues, M.G. Albuquerque, Eur. J. Med. Chem. 46 (2011) 39–51.

[18a] H. Nadri, M. Pirali-Hamedani, M. Shekarchi, M. Abdollahi, V. Sheibani, M. Amanlou, A. Shafiee, A. Foroumadi, Bioorg. Med. Chem. 18 (2010) 6360–6366.

[18b] M. Alipour, M. Khoobi, A. Foroumadi, H. Nadri, A. Moradi, A. Sakhteman, et al., Novel coumarin derivatives bearing N-benzyl pyridinium moiety: potent and dual binding site acetylcholinesterase inhibitors, Bioorg. Med. Chem. 20 (2012) 7214-22.

[18c] M. Alipour, M. Khoobi, H. Nadri, A. Sakhteman, A. Moradi, M. Ghandi, et al., Synthesis of Some New 3-Coumaranone and Coumarin Derivatives as Dual Inhibitors of Acetyl- and Butyrylcholinesterase, Arch. Pharm. Chem. Life Sci. 346 (2013). DOI: 10.1002/ardp.201300080.

[18d] S. F. Razavi, M. Khoobi, H. Nadri, A. Sakhteman, et al., Synthesis and evaluation of 4-substituted coumarins as novel acetylcholinesterase inhibitors, Eur. J. Med. Chem. 64 (2013) 252-259.

[18e] M. Khoobi, M. Alipour, A. Moradi, A. Sakhteman, H. Nadri, et al., Design, synthesis, docking study and biological evaluation of some novel tetrahydrochromeno [3',4':5,6]pyrano[2,3-b]quinolin-6(7H)-one derivatives against acetyl- and butyrylcholinesterase. Eur. J. Med. Chem. In Press. DOI:10.1016/j.ejmech.2013.07.045.

[18f] M. Khoobi, M. Alipour, A. Sakhteman, H. Nadri, A. Moradi, et al., Design, synthesis, biological evaluation and docking study of 5-oxo-4,5-dihydropyrano[3,2-c]chromene derivatives as acetylcholinesterase and butyrylcholinesterase inhibitors. Eur. J. Med. Chem. In Press. DOI: 10.1016/j.ejmech.2013.07.038.

[19] N. Hosseinzadeh, M. Hasani, A. Foroumadi, H. Nadri, S. Emami, N. Samadi, M.A. Faramarzi, P. Saniee, F. Siavoshi, N. Abadian, Y. Mahmoudjanlou, A. Sakhteman, A. Moradi, A. Shafiee, Med. Chem. Res. 22 (2013) 2293–2302.

[20] A. Andreani, S. Burnelli, M. Granaiola, A. Leoni, A. Locatelli, R. Morigi, M. Rambaldi, L. Varoli, L. Landi, C. Prata, F. Vieceli Dalla Sega, C. Caliceti, R.H. Shoemaker, Bioorg. Med. Chem. 18 (2010) 3004–3011.

[21] F. Cheng, W. Li, Y. Zhou, J. Shen, Z. Wu, G. Liu, P.W. Lee, Y. Tang. J. Chem. Inf. Model. 52 (2012) 3099–3105.

[22] G.L. Ellman, K.D. Courtney, V. Andres, R.M. Featherstone, Biochem. Pharmacol. 7 (1961) 88–95.

[23] M.F. Sanner, J. Mol. Graphics Mod. 17 (1999) 57–61.

[24] N.M. O'Boyle, M. Banck, C.A. James, C. Morley, T. Vandermeersch, G.R. Hutchison, J. Cheminform. 3 (2011) 33.

[25] O. Trott, A.J. Olson, J. Comput. Chem. 31 (2010) 455–461.

[26] E.F. Pettersen, T.D. Goddard, C.C. Huang, G.S. Couch, D.M. Greenblatt, E.C. Meng, T.E. Ferrin, J. Comput. Chem. 25 (2004) 1605–1612.

Captions:

Figure 1. Structures of donepezil hydrochloride as a well-known anti-AChE drug, benzofuranone-based compounds reported as AChE-inhibitors and indolinone-based compound as newly designed AChE-inhibitors.

Figure 2. Comparison of the co-crystallized ligand E2020 (red) and its calculated pose (blue) by docking simulation in the active site of AChE. The catalytic site (CS), catalytic anionic subsite (CAS) and peripheral anionic site (PAS) were shown in the receptor.

Figure 3. Representation of the binding mode of the most active compound **3c** in the active site of AChE.

Figure 4. Overlay of the best docked pose of **3c** (green) and **3r** (orange) in the active site of AChE. The catalytic site (CS) and peripheral anionic site (PAS) were also shown for more clarification.

Figure 5. Lineweaver–Burk plots of inhibition kinetics of **3c**: reciprocals of enzyme activity (*eel*AChE) vs. reciprocals of substrate (acetylthiocholine) concentration in the presence of different concentrations of inhibitor **3c**.

Figure 6. The plot of Lineweaver–Burk plots slopes vs. inhibitor concentrations

Scheme 1. Synthesis of (*E*)-1-benzyl-4-((2-oxoindolin-3-ylidene)methyl)pyridinium halide derivatives **3a-u**. *Reagents and conditions*: (i) pyridine-4-carboxaldehyde, PTSA, toluene, reflux (ii) benzyl halide derivatives, acetonitrile, 60-70 ºC.

Table 1. Chemical structure data, AChE and BuChE inhibitory activities of compounds **3a-u**.

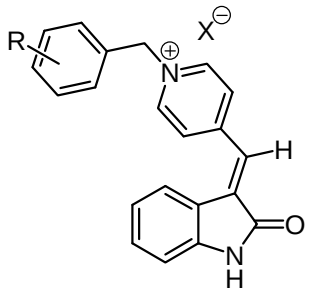

Compound	R	X	IC_{50} (nM)[a] AChE	IC_{50} (nM) BuChE	Selectivity for AChE [b]
3a	H	Br	47.10 ± 0.41	4300 ± 298	91.3
3b	2-F	Cl	1.25 ± 0.017	4270 ± 295	3416
3c	2-Cl	Cl	0.44 ± 0.006	1370 ± 94	3113
3d	2-CH_3	Cl	15.3 ± 0.29	887 ± 61	57.9
3e	2-Br	Cl	1.46 ± 0.013	1230 ± 85	842.5
3f	2-NO_2	Br	214 ± 1.87	1600 ± 111	7.5
3g	2-Cl,6-F	Cl	4.1 ± 0.036	2000 ± 138	487.8
3h	2,6-Cl_2	Cl	17 ± 0.15	1500 ± 104	88.2
3i	3-Cl	Br	4.9 ± 0.043	1350 ± 94	275.5
3j	3-Br	Cl	10.3 ± 0.09	1740 ± 121	169
3k	3-CH_3	Cl	5.2 ± 0.045	1700 ± 118	327
3l	3-OCH_3	Cl	6.6 ± 0.058	2800 ± 194	424.2
3m	3-F	Cl	12.8 ± 0.11	4500 ± 312	351.5
3n	4-F	Cl	677 ± 5.9	3100 ± 215	4.58
3o	4-Cl	Cl	590 ± 5.15	2200 ± 152	3.73
3p	4-Br	Cl	653.4 ± 5.7	1900 ± 132	2.9
3q	4-OCH_3	Cl	677 ± 5.91	7900 ± 547	11.67
3r	4-NO_2	Cl	744 ± 6.49	7500 ± 520	10
3s	3,4-Cl_2	Cl	29.4 ± 0.26	3300 ± 227	112.2
3t	2,4-Cl_2	Cl	257.6 ± 2.25	2500 ± 174	9.7
3u	4-CH_2Cl	Cl	103.4 ± 0.90	1000 ± 69	9.67
Donepezil			14 ± 0.8	5380 ± 340	384.3

[a] Data are expressed as Mean ± S.E. of at least three different experiments.
[b] Selectivity for AChE = IC_{50} (BuChE)/IC_{50} (AChE).

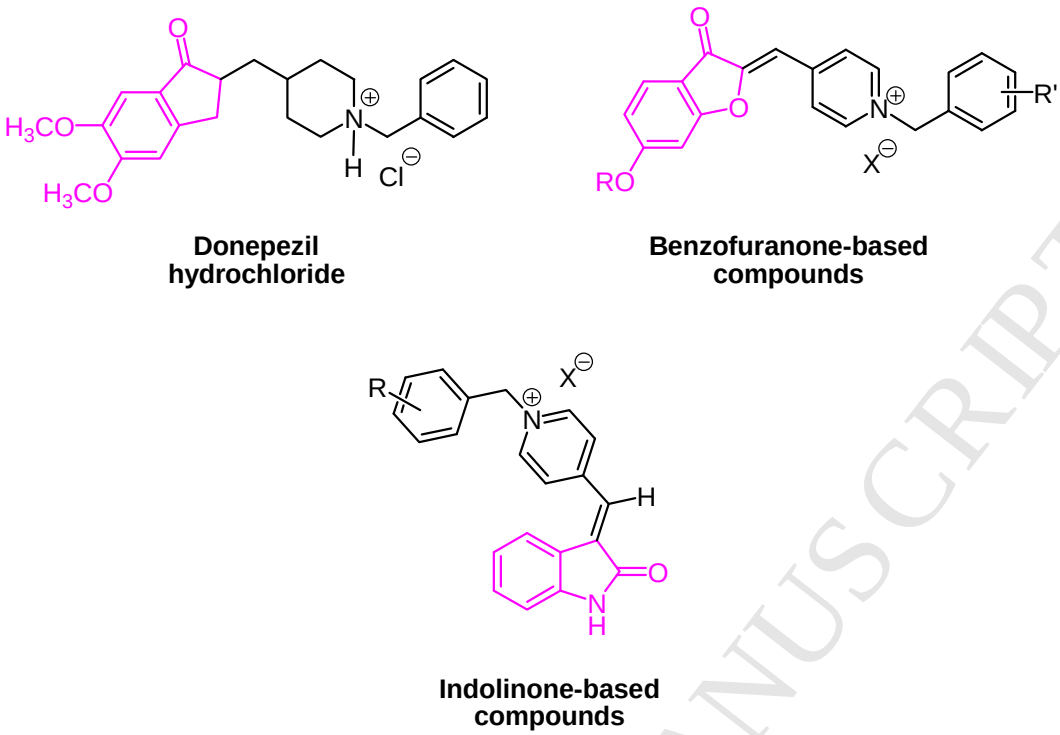

Figure 1. Structures of donepezil hydrochloride as a well-known anti-AChE drug, benzofuranone-based compounds reported as AChE-inhibitors and indolinone-based compound as newly designed AChE-inhibitors.

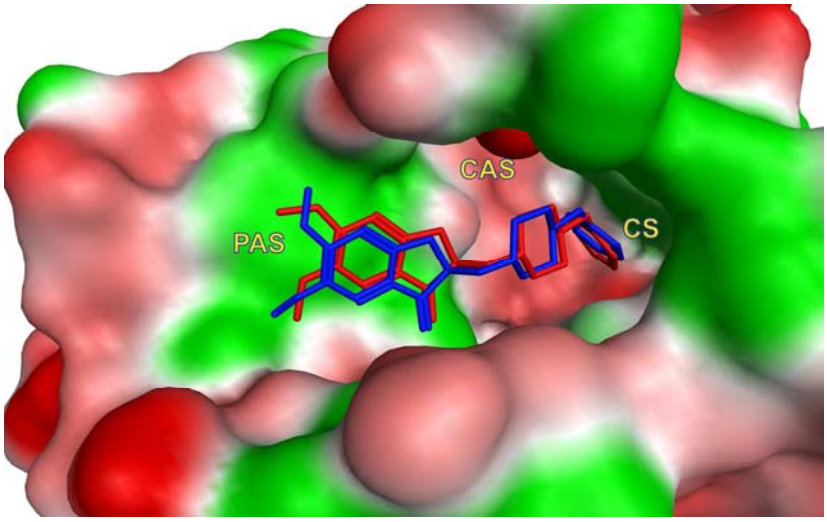

Figure 2. Comparison of the co-crystallized ligand E2020 (red) and its calculated pose (blue) by docking simulation in the active site of AChE. The catalytic site (CS), catalytic anionic subsite (CAS) and peripheral anionic site (PAS) were shown in the receptor.

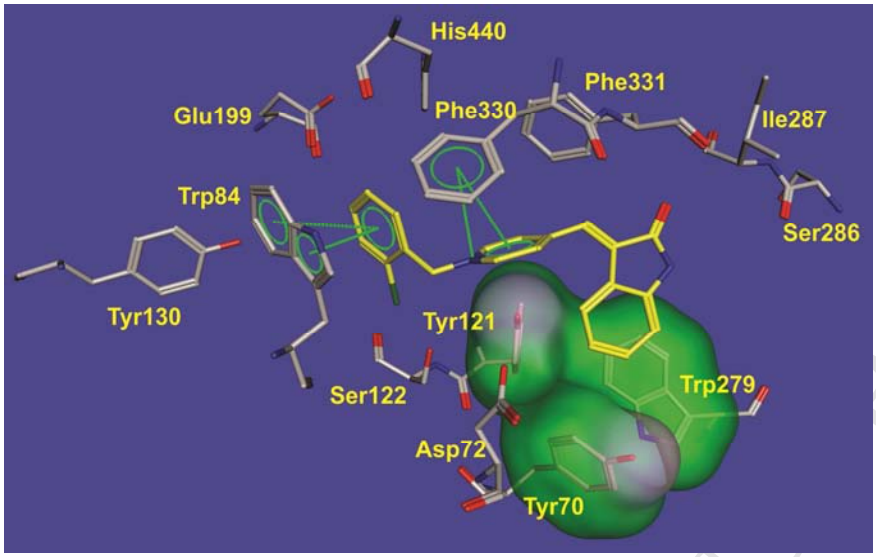

Figure 3. Representation of the binding mode of the most active compound **3c** in the active site of AChE.

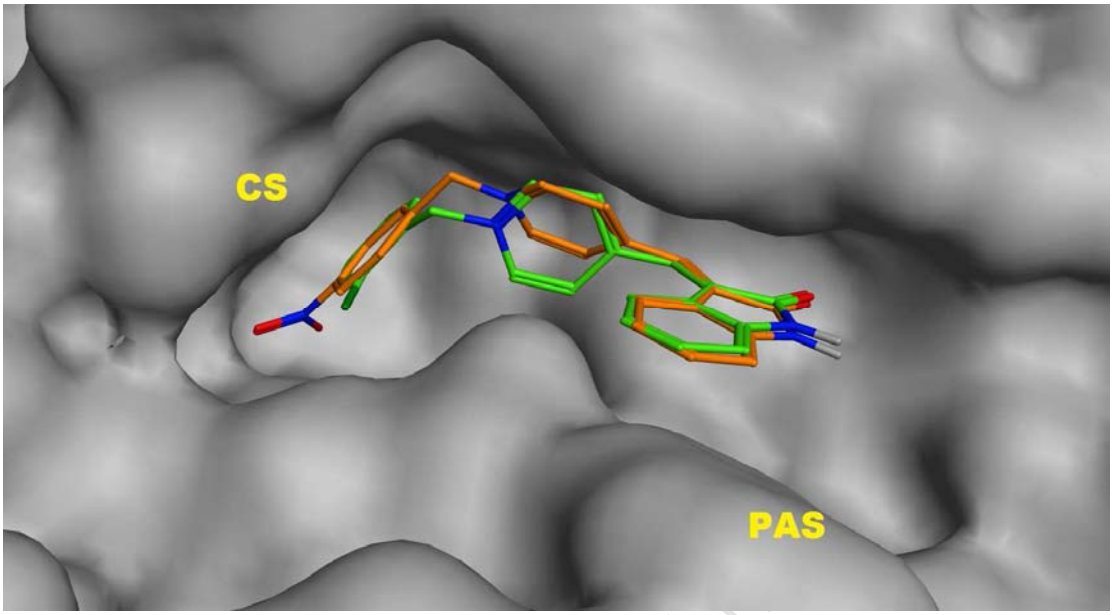

Figure 4. Overlay of the best docked pose of **3c** (green) and **3r** (orange) in the active site of AChE. The catalytic site (CS) and peripheral anionic site (PAS) were also shown for more clarification.

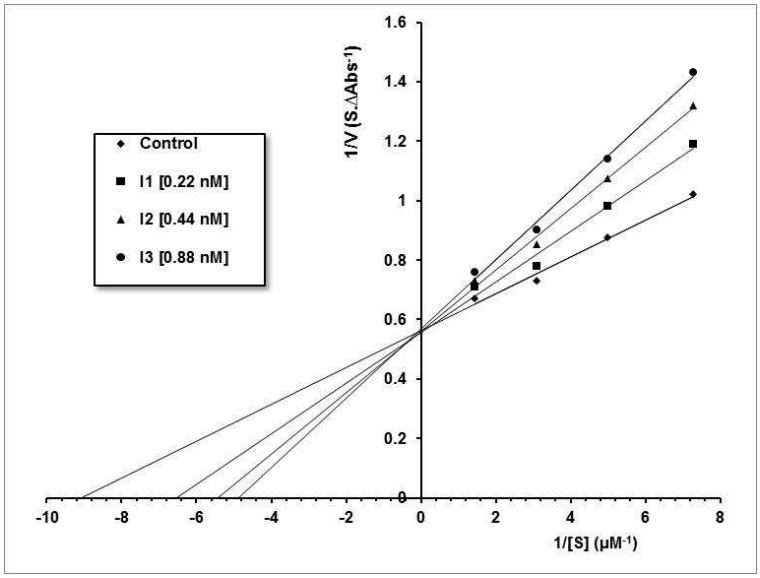

Figure 5. Lineweaver–Burk plots of inhibition kinetics of **3c**: reciprocals of enzyme activity (*eel*AChE) vs. reciprocals of substrate (acetylthiocholine) concentration in the presence of different concentrations of inhibitor **3c**.

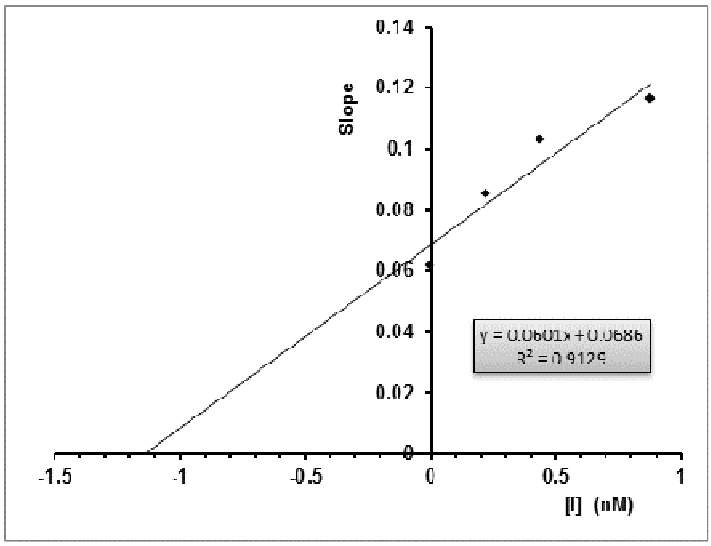

Figure 6. The plot of Lineweaver–Burk plots slopes vs. inhibitor concentrations

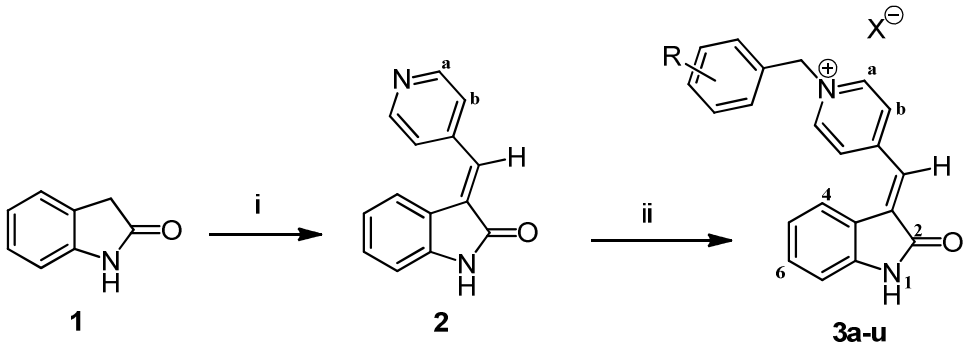

Scheme 1. Synthesis of (*E*)-1-benzyl-4-((2-oxoindolin-3-ylidene)methyl)pyridinium halide derivatives **3a-u**. *Reagents and conditions*: (i) pyridine-4-carboxaldehyde, PTSA, toluene, reflux (ii) benzyl halide derivatives, acetonitrile, 60-70 ºC.

Research Highlights

► Indolinone-based compounds were designed as dual-binding inhibitors of AChE.

► 2-Chlorobenzyl analog **3c** was 32-fold more potent than donepezil as standard drug.

► Also, most compounds showed potent anti-AChE activity superior to donepezil.

► Docking study showed that indoline binds to PAS and pyridinium binds to CAS.

Supplementary material

Indolinone-based acetylcholinesterase inhibitors: synthesis, biological activity and molecular modeling

Hamidreza Akrami, Bibi Fatemeh Mirjalili, Mehdi Khoobi, Hamid Nadri, Alireza Moradi, Amirhossein Sakhteman, Saeed Emami, Alireza Foroumadi, Abbas Shafiee

Table 1. Condensation of oxindole (1mmol) and pyridine-4-carbaldehyde (1mmol) under various conditions

Entry	Catalyst	Solvent condition	Time(h)	Yield%(E/Z)*
1	H_2SO_4 (20 mol-%)	Solvent free/50–60 ^oC	5	(55/45)
2	H_2SO_4 (20 mol-%)	reflux/CH_2Cl_2	10	(55/45)
3	$Zr(HSO_4)_4$ (20 mol-%)	reflux/toluene	6	(50/50)
4	I_2	r.t/CH2Cl2	7	(50/50)
5	$MgSO_4$	Solvent free, 60 ^oC	6	(55/45)
6	Silica sulfuric acid	Solvent free, 80 ^oC	5	(55/45)
7	LiOH	r.t/Ethanol	8	(60/40)
8	PTSA	Solvent free, 80 ^oC	6	(60/40)
9	PTSA	reflux/acetonitrile	5	(70/30)
10	PTSA	reflux/diethyl ether	9	(55/45)
11	PTSA	reflux/toluene	3	(90/10)

*The crude product was monitored by NMR

Table 2. Reaction of (*E*)-3-(pyridin-4-ylmethylene)indolin-2-one **(2)** (1 mmol) with benzyl bromide (1.5 mmol)

entry	solvent Condition	Time	Yield %
1	reflux/toluene	5	75-80
2	reflux/diethyl ether	7	70-75
3	reflux/ acetonitrile	6	75-80
4	reflux/ethanol:H_2O	5	65-70
5	r.t/ toluene	10	85-90
6	r.t/ acetonitrile	10	95-100

Spectroscopic data

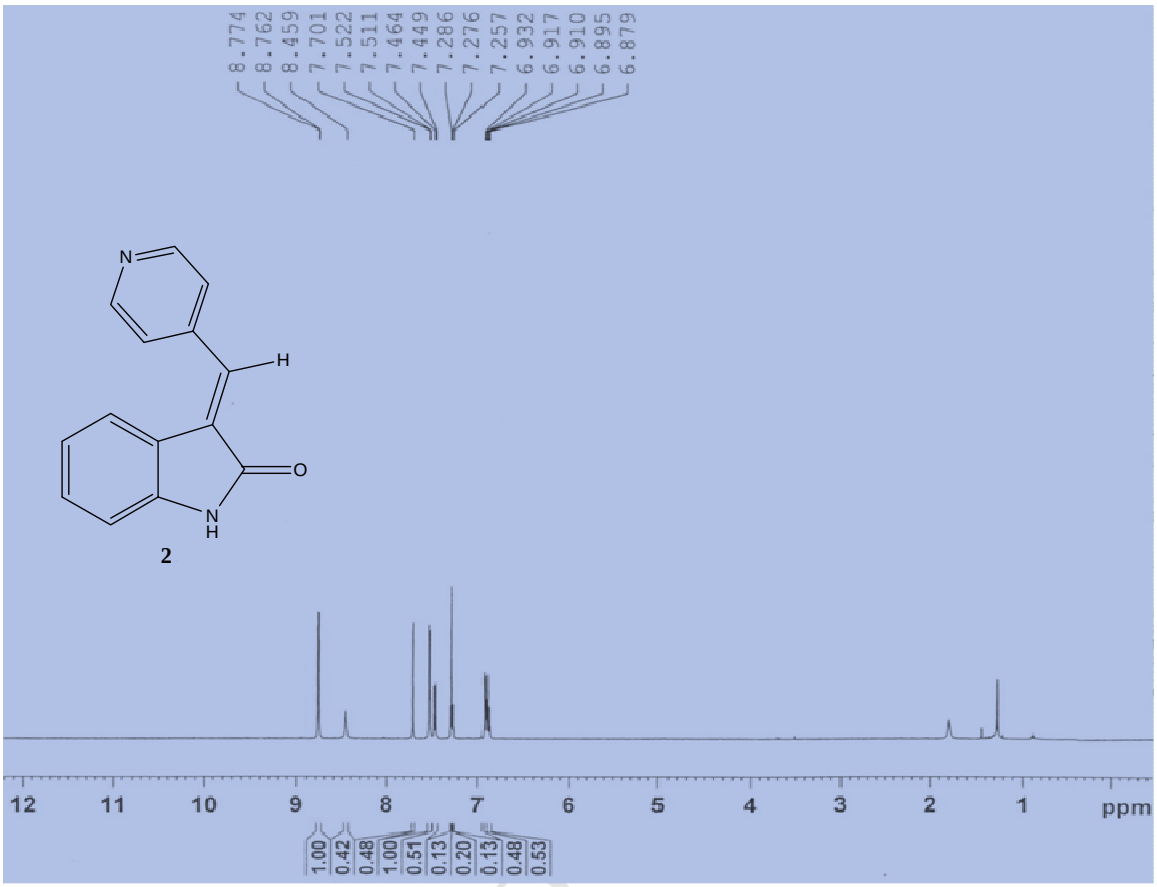

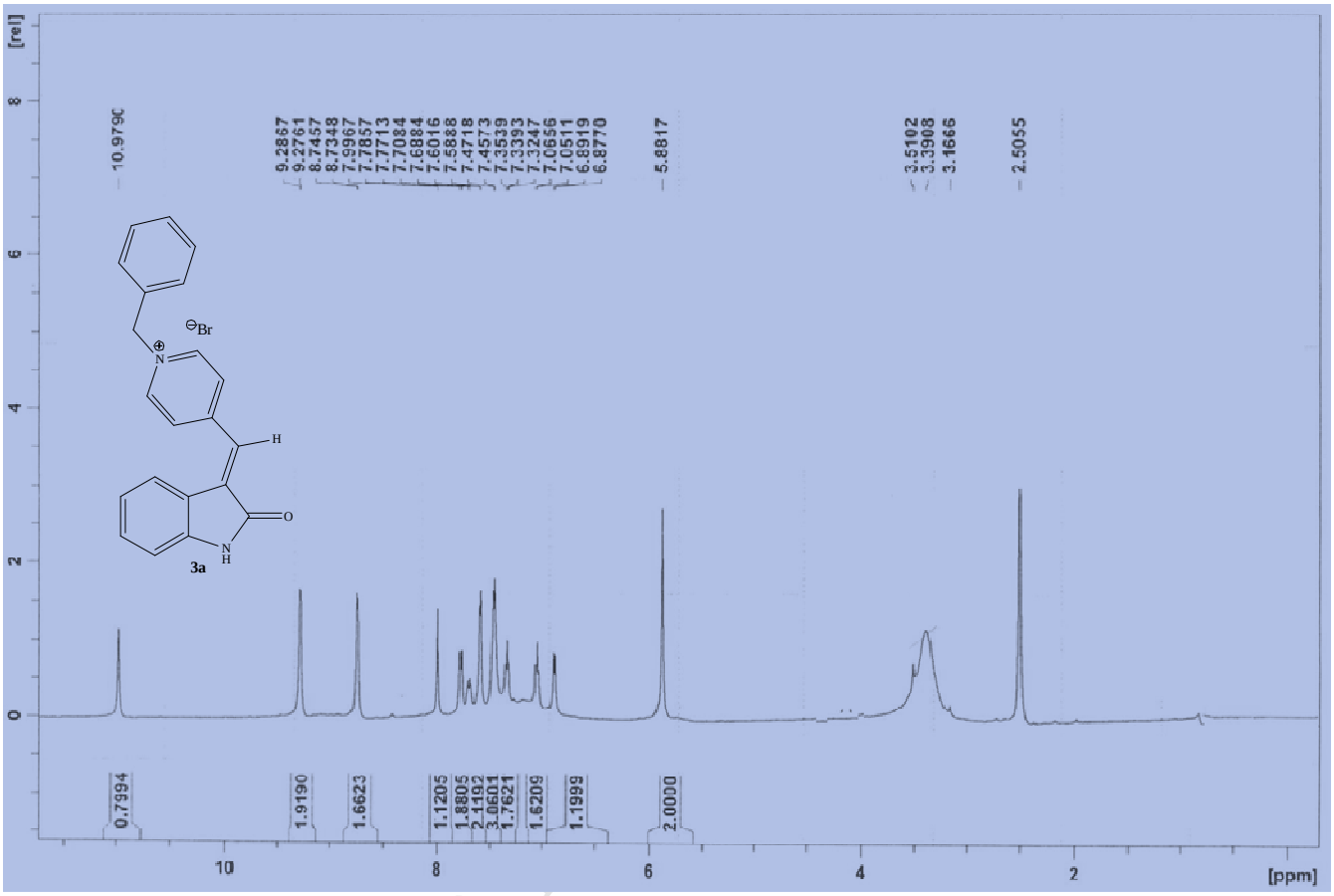

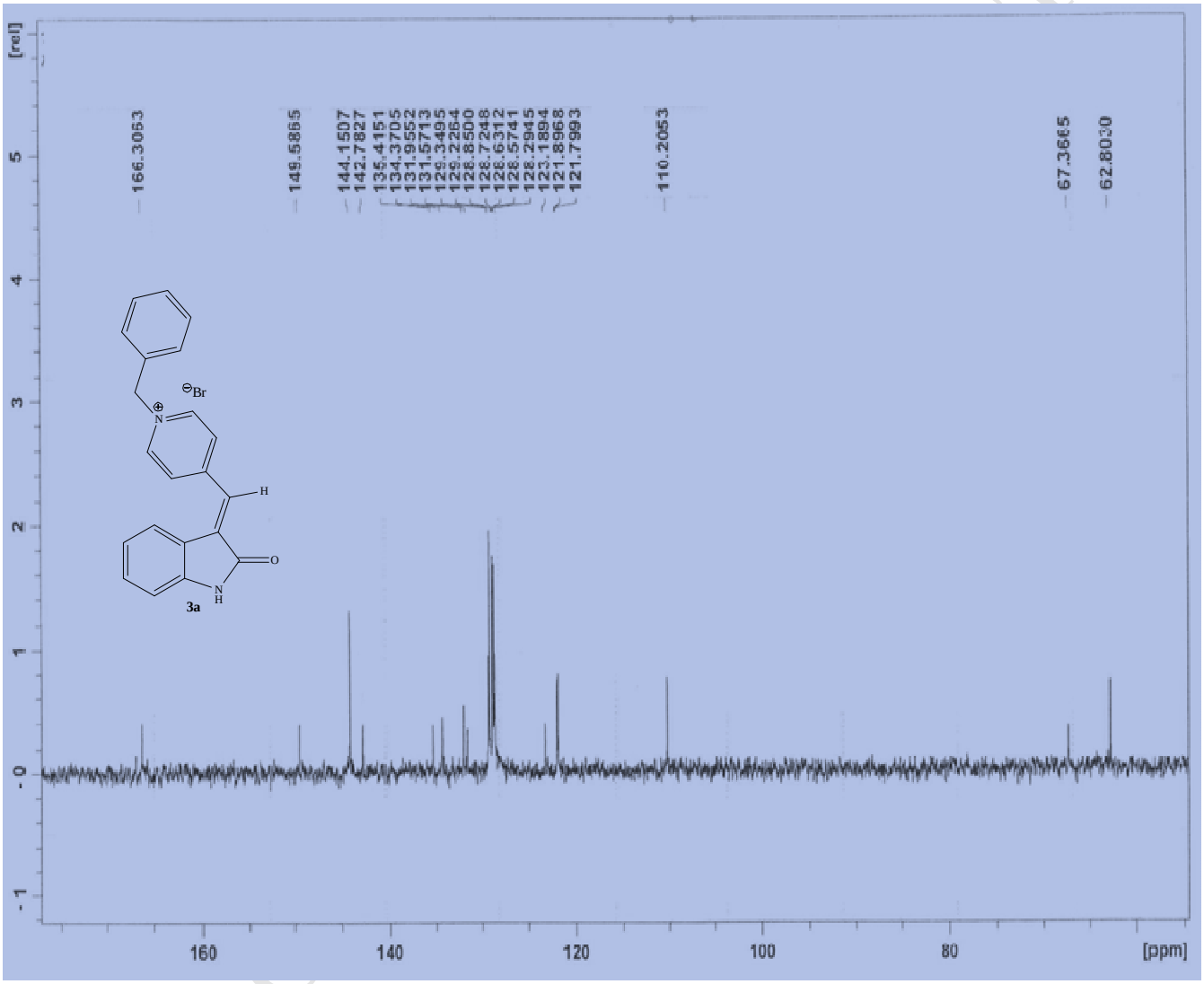
[rel]
166.3053
149.5865
144.1507
142.7827
135.4151
134.3705
131.9552
131.5713
131.3495
129.2264
128.8500
126.7248
126.6312
126.5741
126.2945
123.1894
121.8968
121.7993
110.2053
67.3665
62.8030
Br
H
O
N
H
3a
160
140
120
100
80
[ppm]

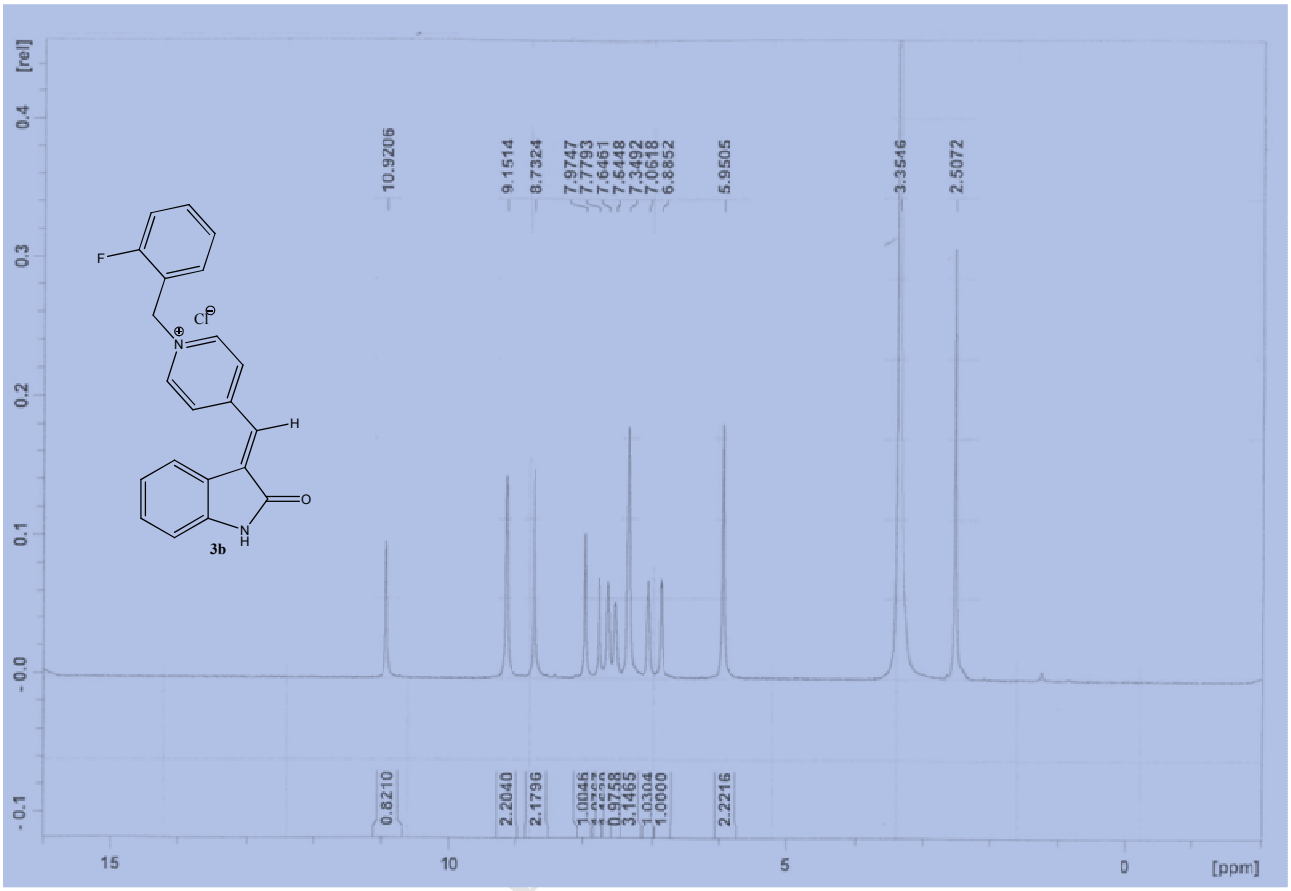

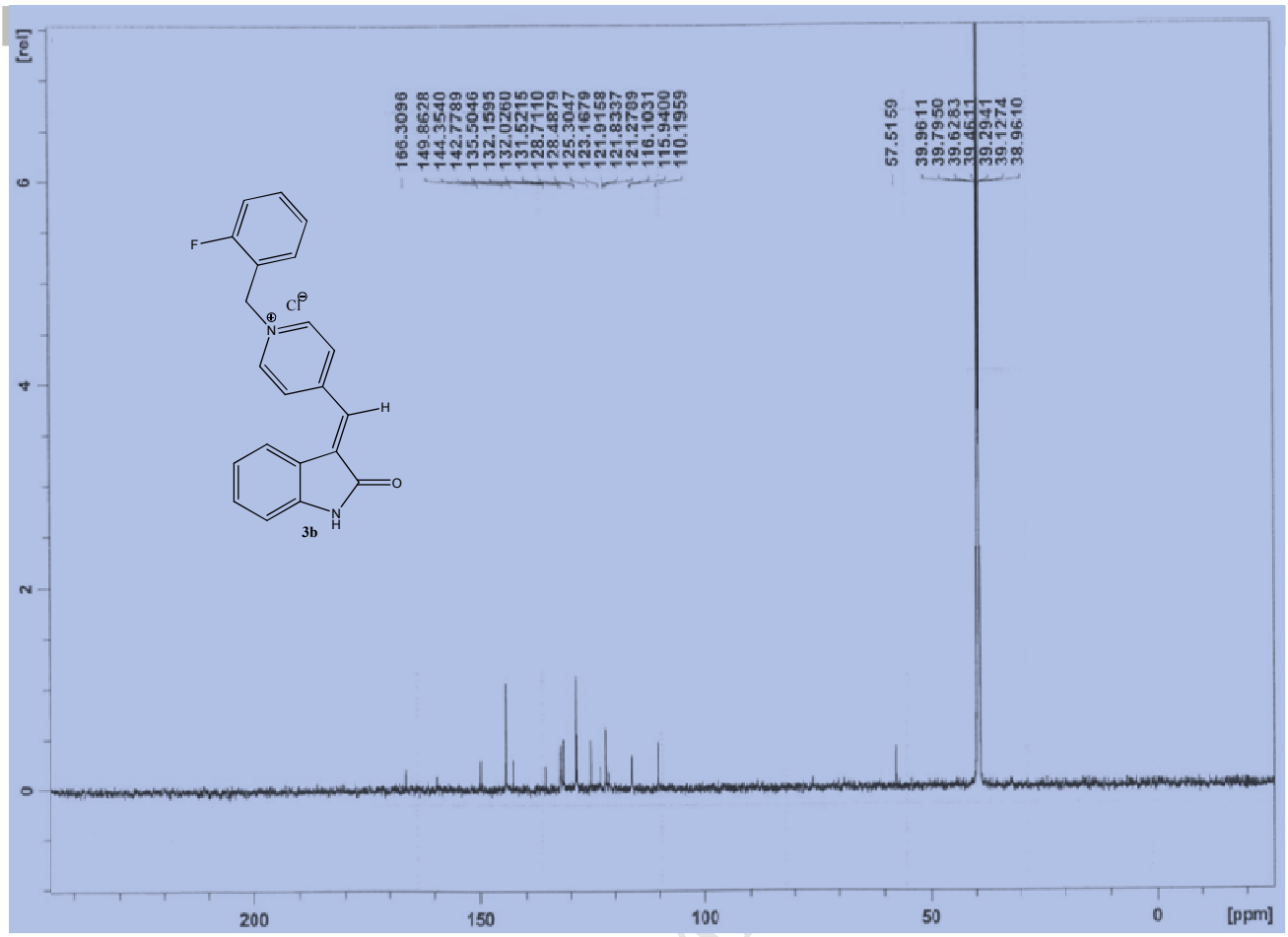

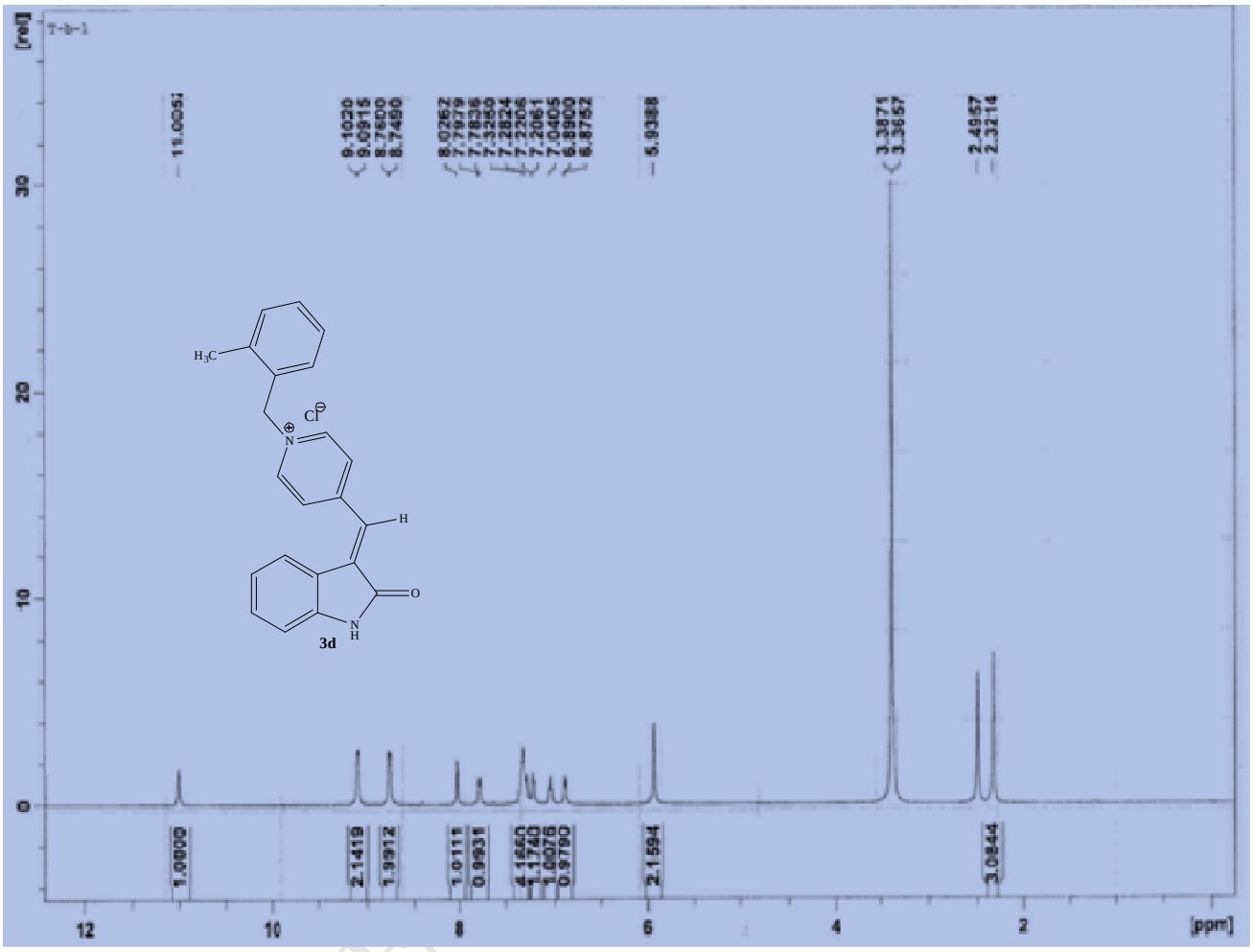
[rel]
T-b-1
11.0051
9.1020
9.0915
8.7600
8.7490
8.0262
7.7979
7.7836
7.3350
7.2824
7.2706
7.2061
7.0405
6.8900
6.8752
5.9388
3.3871
3.3657
2.4957
2.3214
1.0000
2.1419
1.9312
1.0111
0.9931
4.1660
1.1740
1.0078
0.9790
2.1594
3.0844
[ppm]

3d

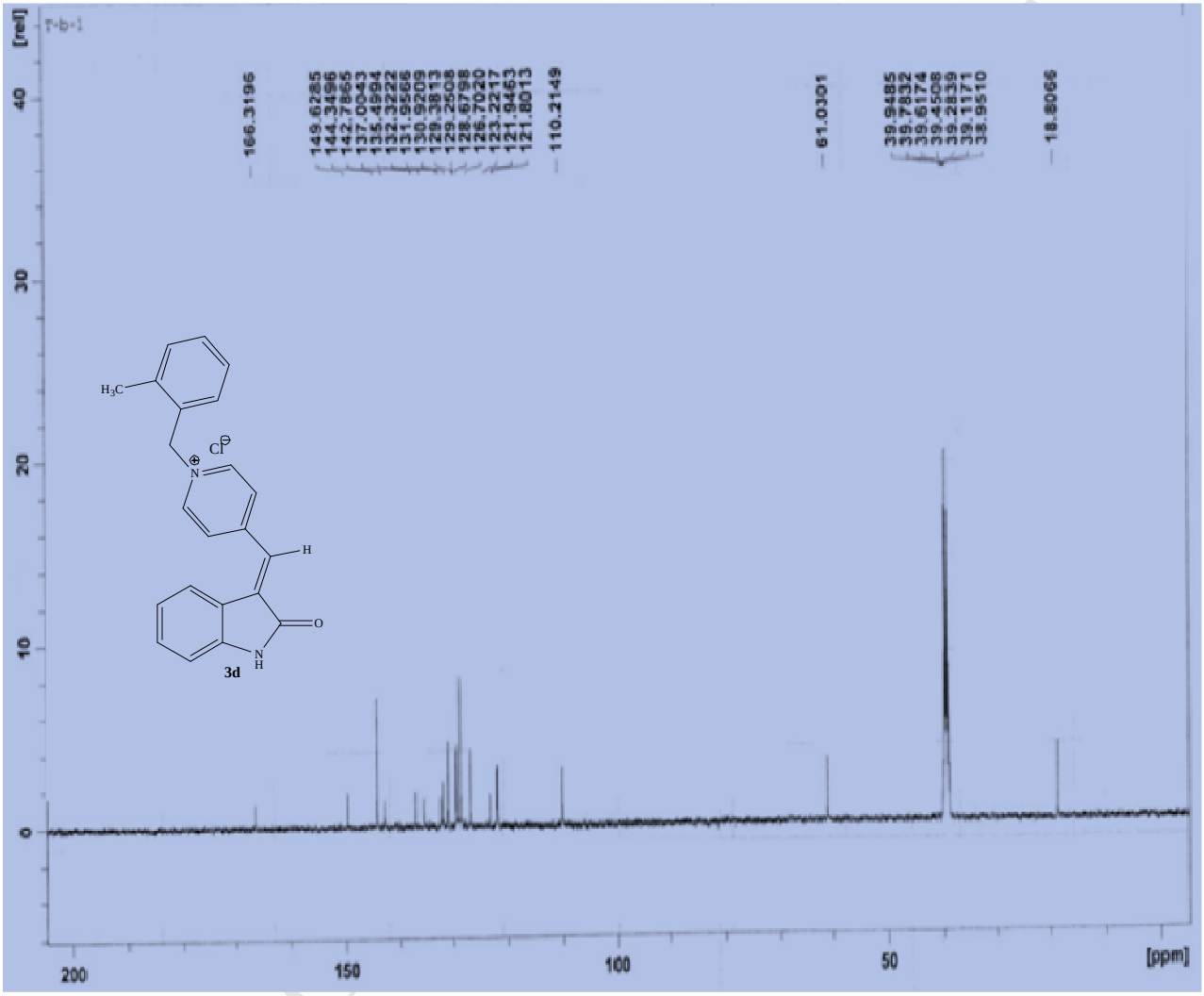
[rel]
40
30
20
10
0
166.3196
149.6265
144.3496
142.7865
137.0043
135.4594
132.3222
131.9566
130.9209
129.3813
129.2508
128.6798
126.7020
123.2217
121.9465
121.8013
110.2149
61.0301
39.9485
39.7832
39.6174
39.4508
39.2839
39.1171
38.9510
18.8066
200
150
100
50
[ppm]
H3C
Cl
N
H
O
N
H
3d

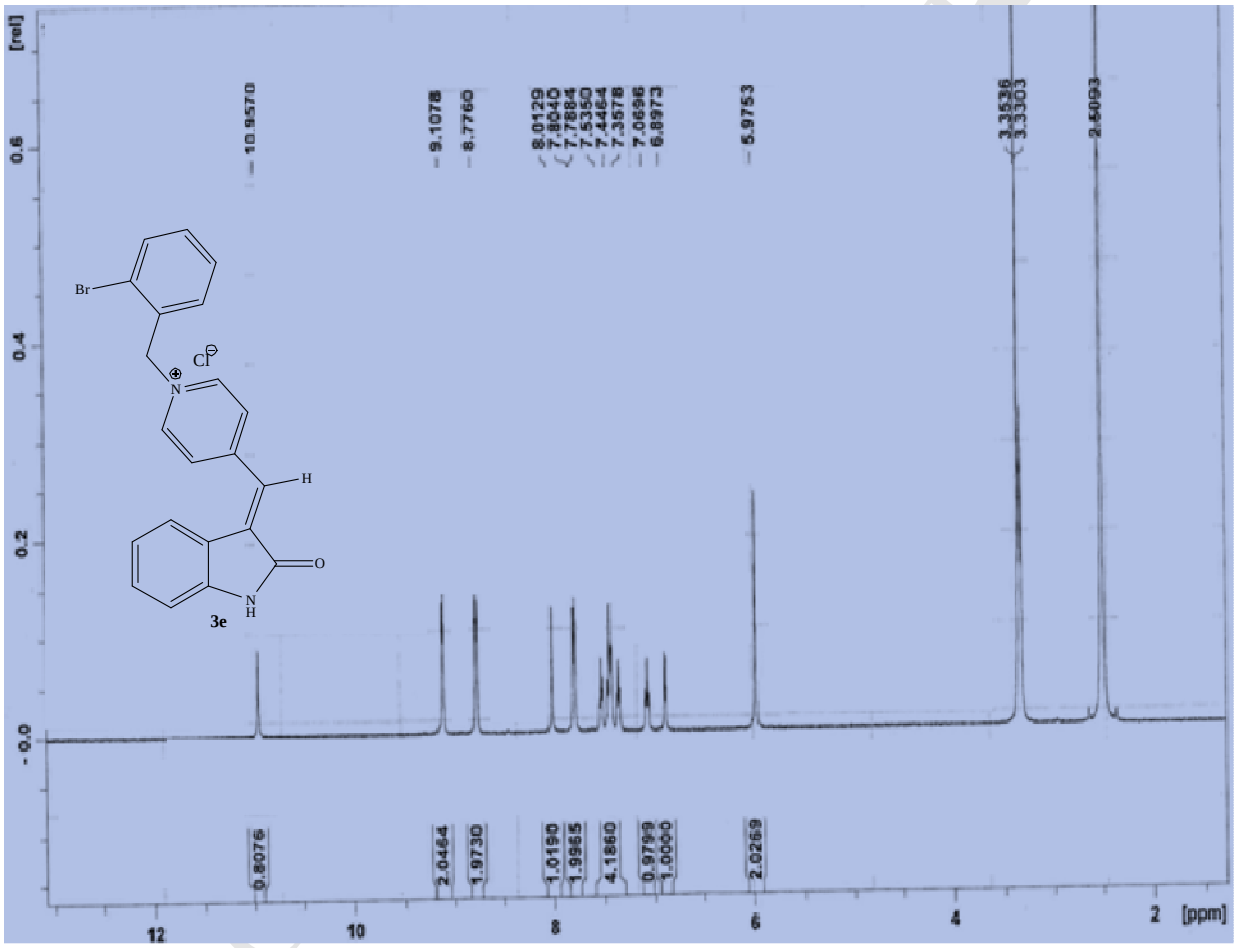
[rel]
0.6
0.4
0.2
-0.0
10.9570
9.1078
8.7760
8.0129
7.8045
7.7884
7.5350
7.4464
7.3578
7.0696
6.8973
5.9753
3.3536
3.3303
2.5093
0.8076
2.0464
1.9730
1.0190
1.9965
4.1860
0.9799
1.0000
2.0269
12
10
8
6
4
2
[ppm]
Br
Cl
N
H
O
N
H

3e

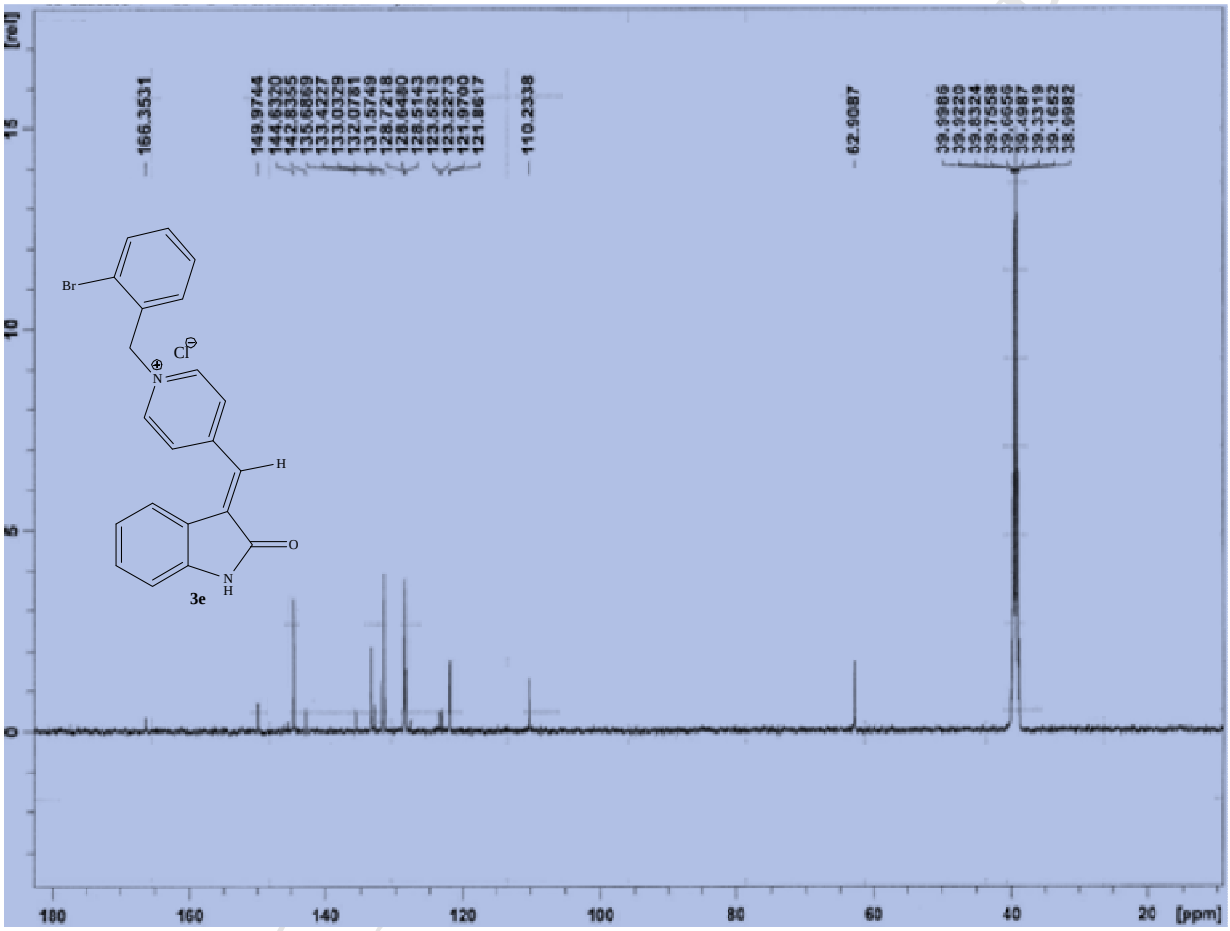
166.3531
149.9744
144.6320
142.8355
135.6869
133.4277
133.0329
132.0761
131.5749
128.7218
128.6480
128.5143
123.5213
123.2273
121.9700
121.8617
110.2338
62.9087
39.9986
39.9220
39.8324
39.7558
39.6656
39.4987
39.3318
39.1652
38.9982
[rel]
15
10
5
0
180
160
140
120
100
80
60
40
20
[ppm]
Br
Cl
N
H
O
N
H
3e

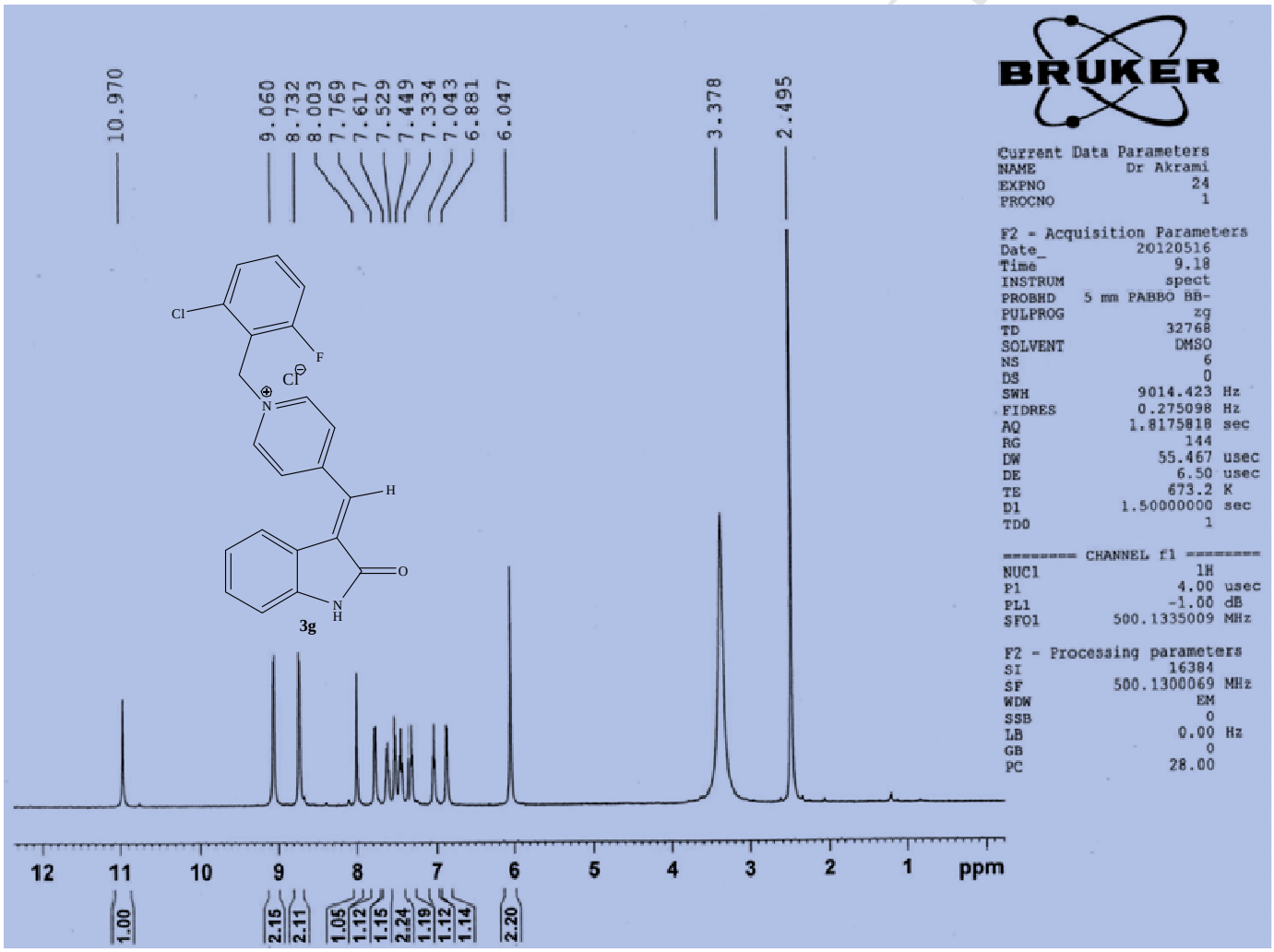
10.970
9.060
8.732
8.003
7.769
7.617
7.529
7.449
7.334
7.043
6.881
6.047
3.378
2.495
Cl
F
Cl
N
H
O
N
H
3g
BRUKER
Current Data Parameters
NAME Dr Akrami
EXPNO 24
PROCNO 1
F2 - Acquisition Parameters
Date_ 20120516
Time 9.18
INSTRUM spect
PROBHD 5 mm PABBO BB-
PULPROG zg
TD 32768
SOLVENT DMSO
NS 6
DS 0
SWH 9014.423 Hz
FIDRES 0.275098 Hz
AQ 1.8175818 sec
RG 144
DW 55.467 usec
DE 6.50 usec
TE 673.2 K
D1 1.50000000 sec
TD0 1
======== CHANNEL f1 ========
NUC1 1H
P1 4.00 usec
PL1 -1.00 dB
SFO1 500.1335009 MHz
F2 - Processing parameters
SI 16384
SF 500.1300069 MHz
WDW EM
SSB 0
LB 0.00 Hz
GB 0
PC 28.00
12
11
10
9
8
7
6
5
4
3
2
1
ppm
1.00
2.15
2.11
1.05
1.12
1.15
2.24
1.19
1.12
1.14
2.20

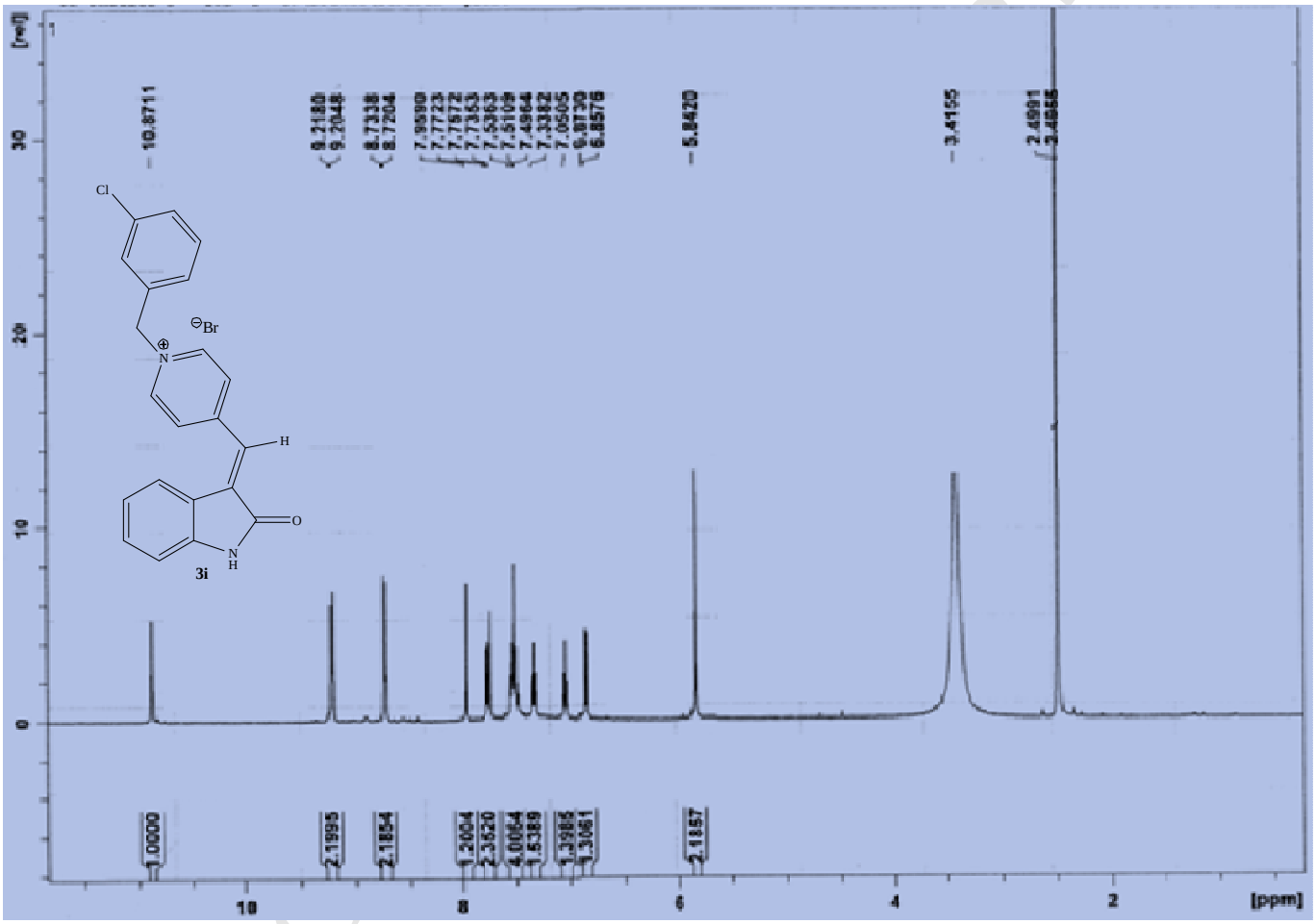
10.8711
9.2180
9.2044
8.7338
8.7204
7.9990
7.7723
7.7572
7.7353
7.5963
7.5109
7.4964
7.3382
7.0505
6.8739
6.8578
5.8420
3.4155
2.4991
3.4888
Cl
Br
N
H
O
N
H
3i
1.0000
2.1995
2.1854
1.3094
2.3520
4.0084
1.5389
1.3988
1.3061
2.1857
10
8
6
4
2
[ppm]

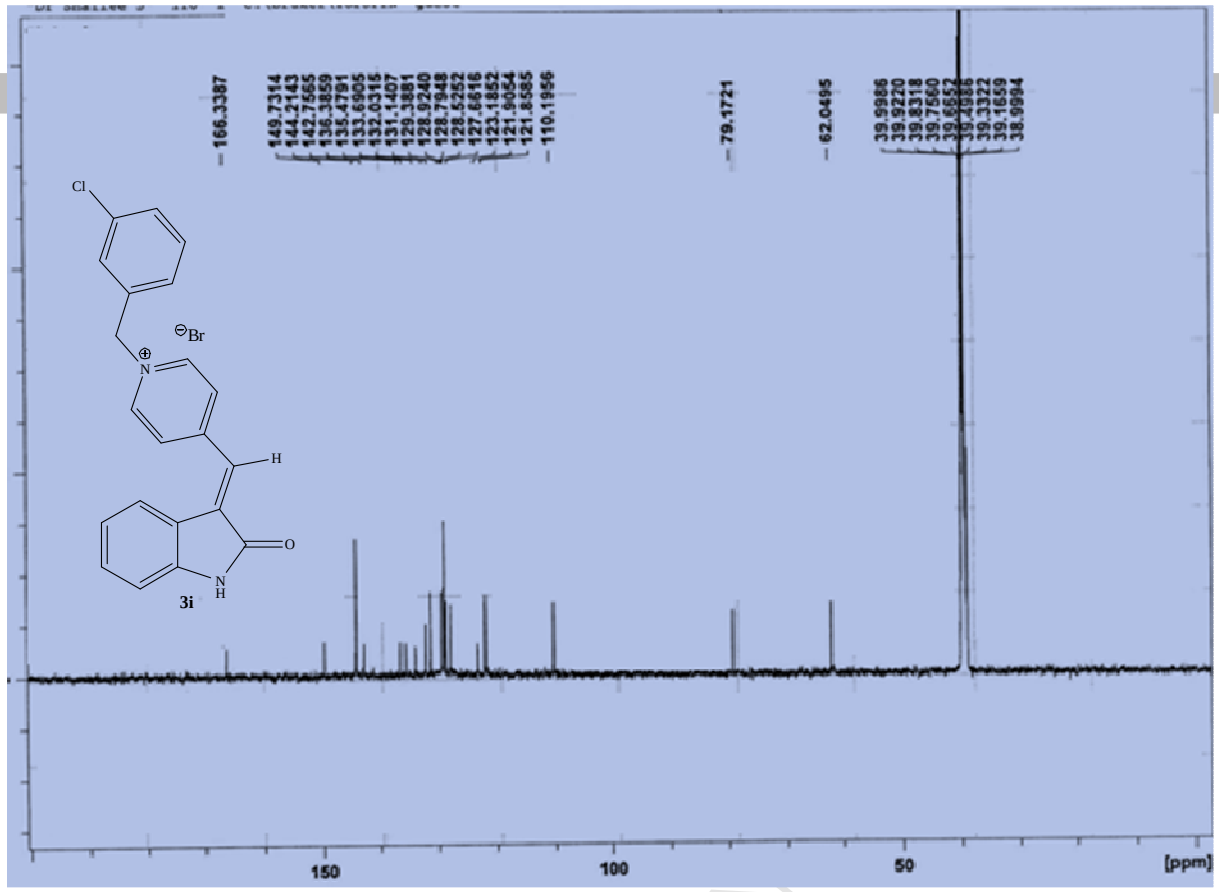

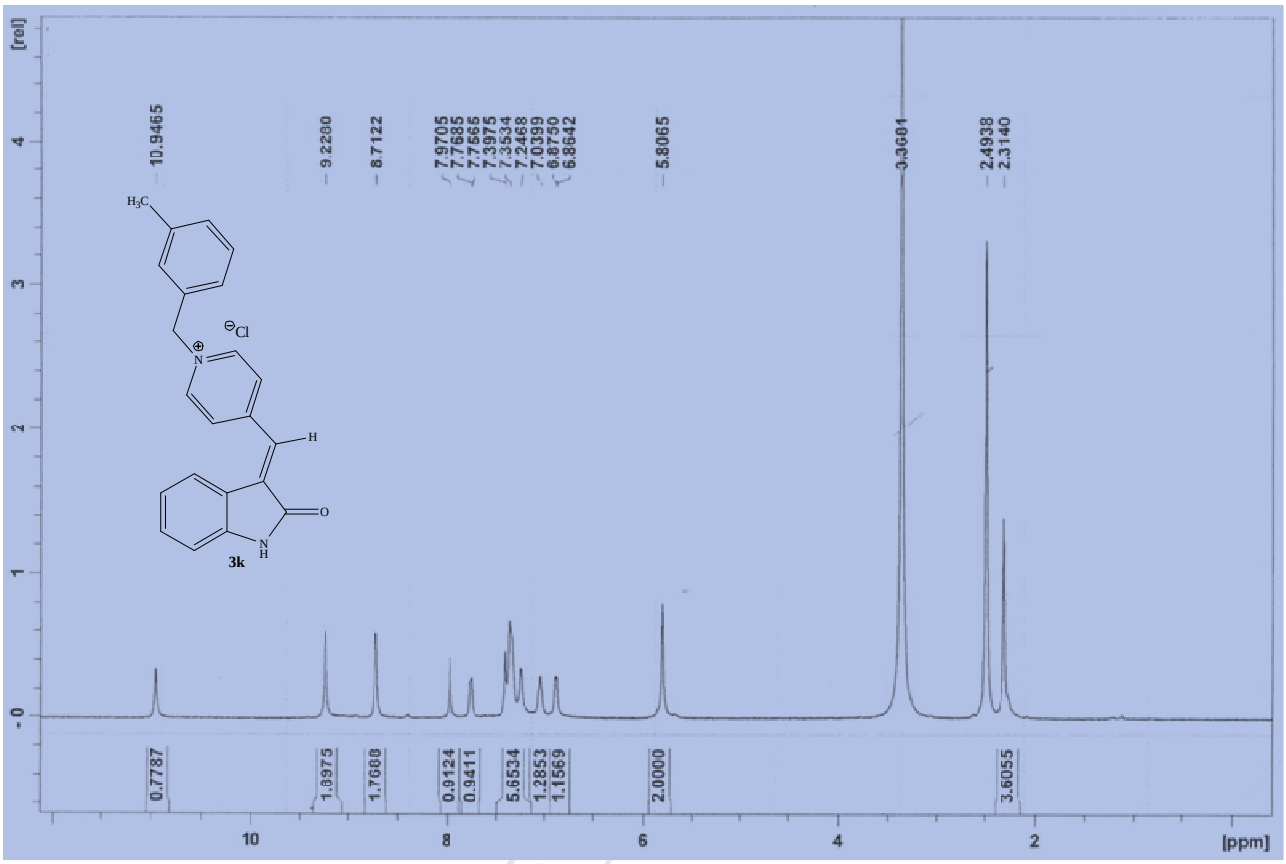

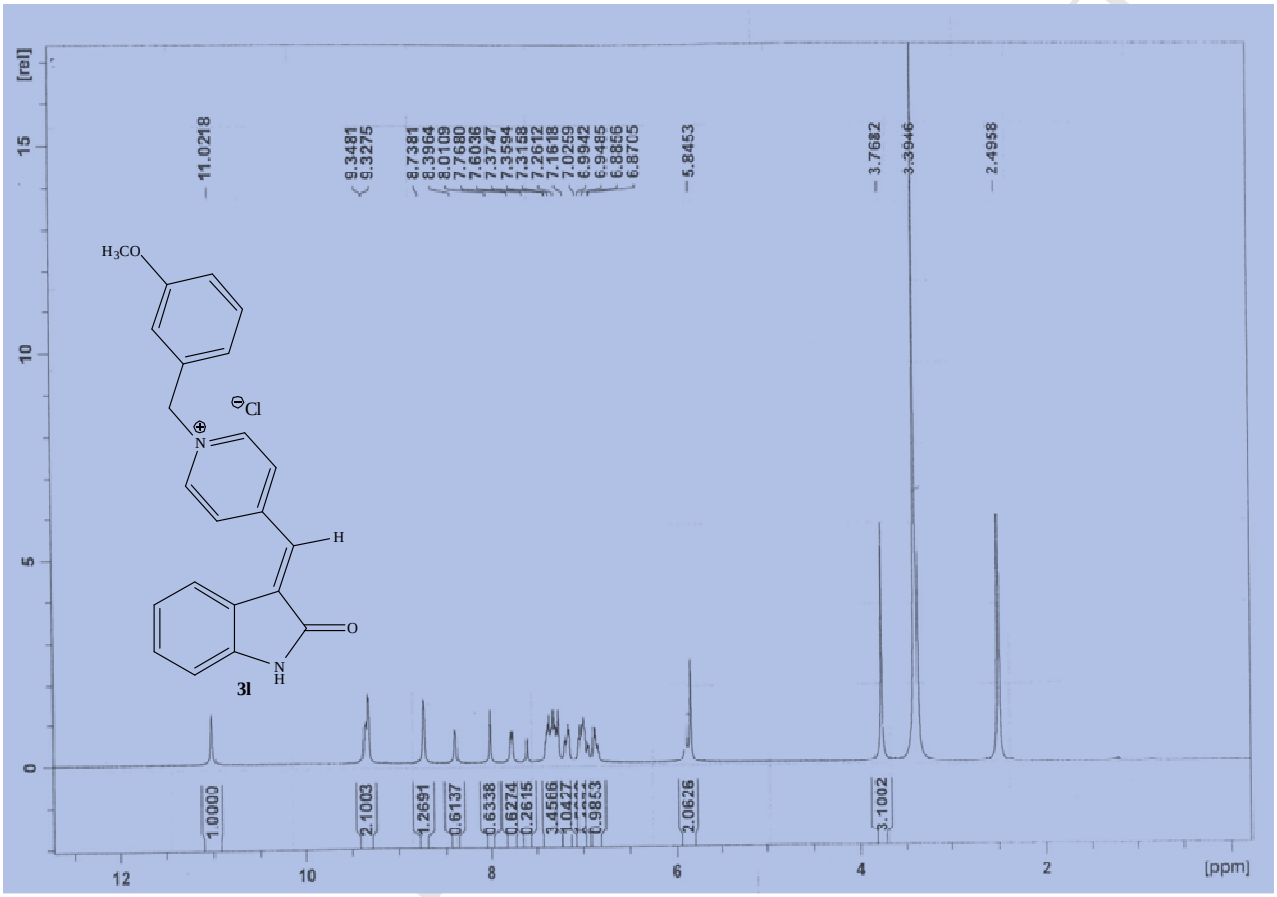
[rel]
15
10
5
0
11.0218
9.3481
9.3275
8.7381
8.3964
8.0109
7.7680
7.6036
7.3747
7.3594
7.3158
7.2612
7.1618
7.0259
6.9942
6.9485
6.8856
6.8705
5.8453
3.7682
3.3946
2.4958
1.0000
2.1003
1.2691
0.6137
0.6338
0.6274
0.2615
3.4566
1.0427
0.9853
2.0626
3.1002
12
10
8
6
4
2
[ppm]
H3CO
Cl
N
H
O
N
H
3l

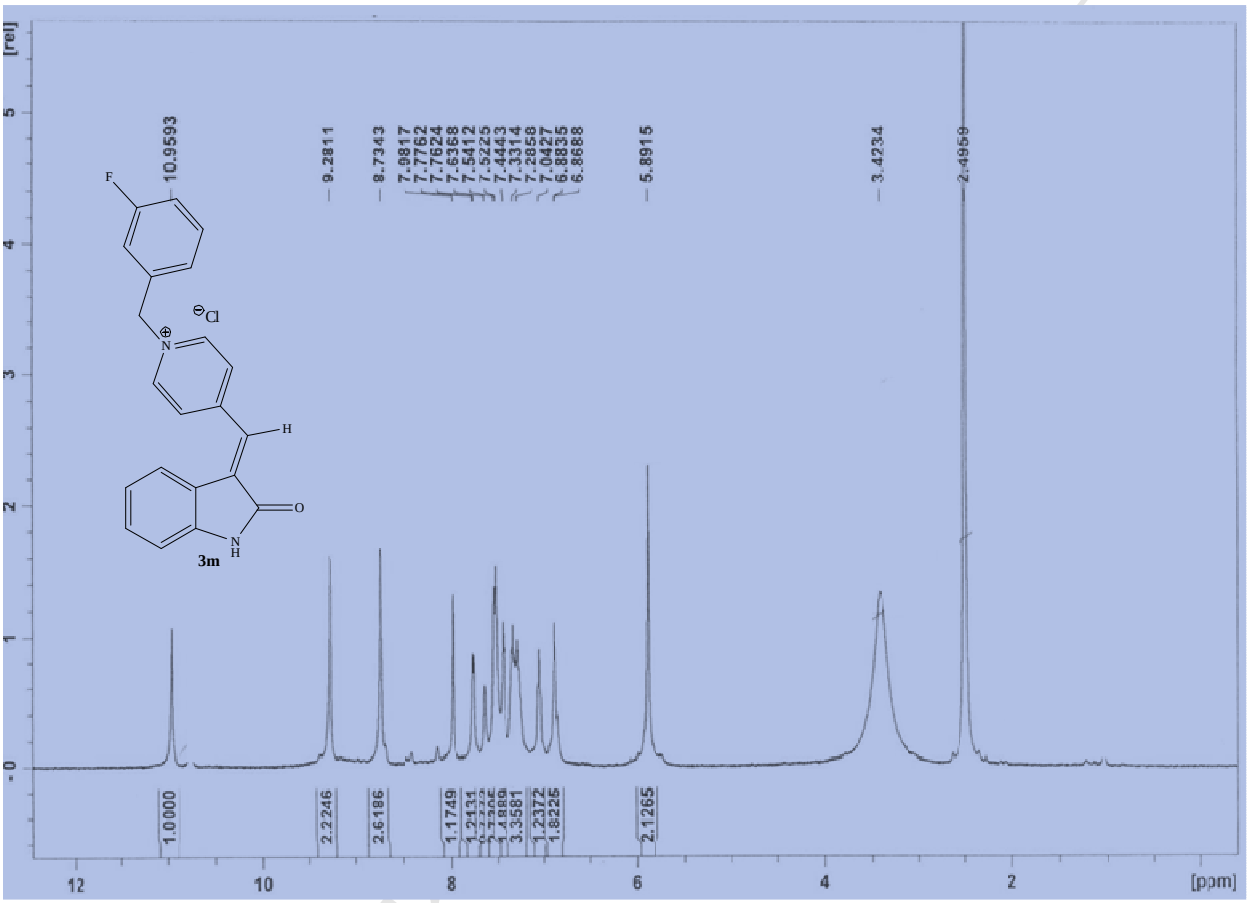
10.9593
9.2811
8.7343
7.9817
7.7762
7.7624
7.6368
7.5412
7.5225
7.4443
7.3314
7.2858
7.0427
6.8835
6.8688
5.8915
3.4234
2.4959
F
Cl
N
H
O
N
H
3m
[rel]
5
4
3
2
1
0
1.0000
2.2246
2.6186
1.1749
3.3581
1.2372
1.8225
2.1265
12
10
8
6
4
2
[ppm]

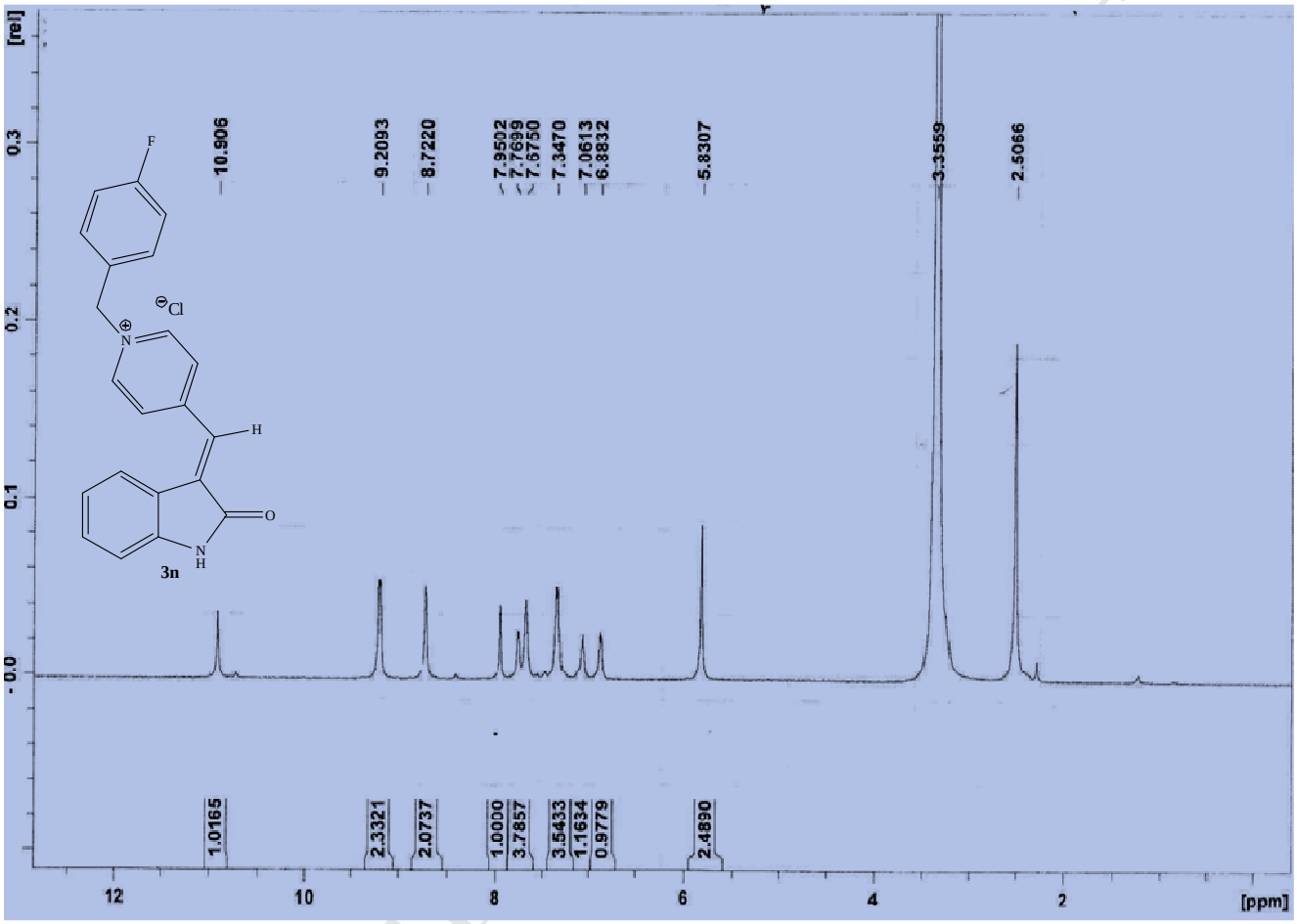

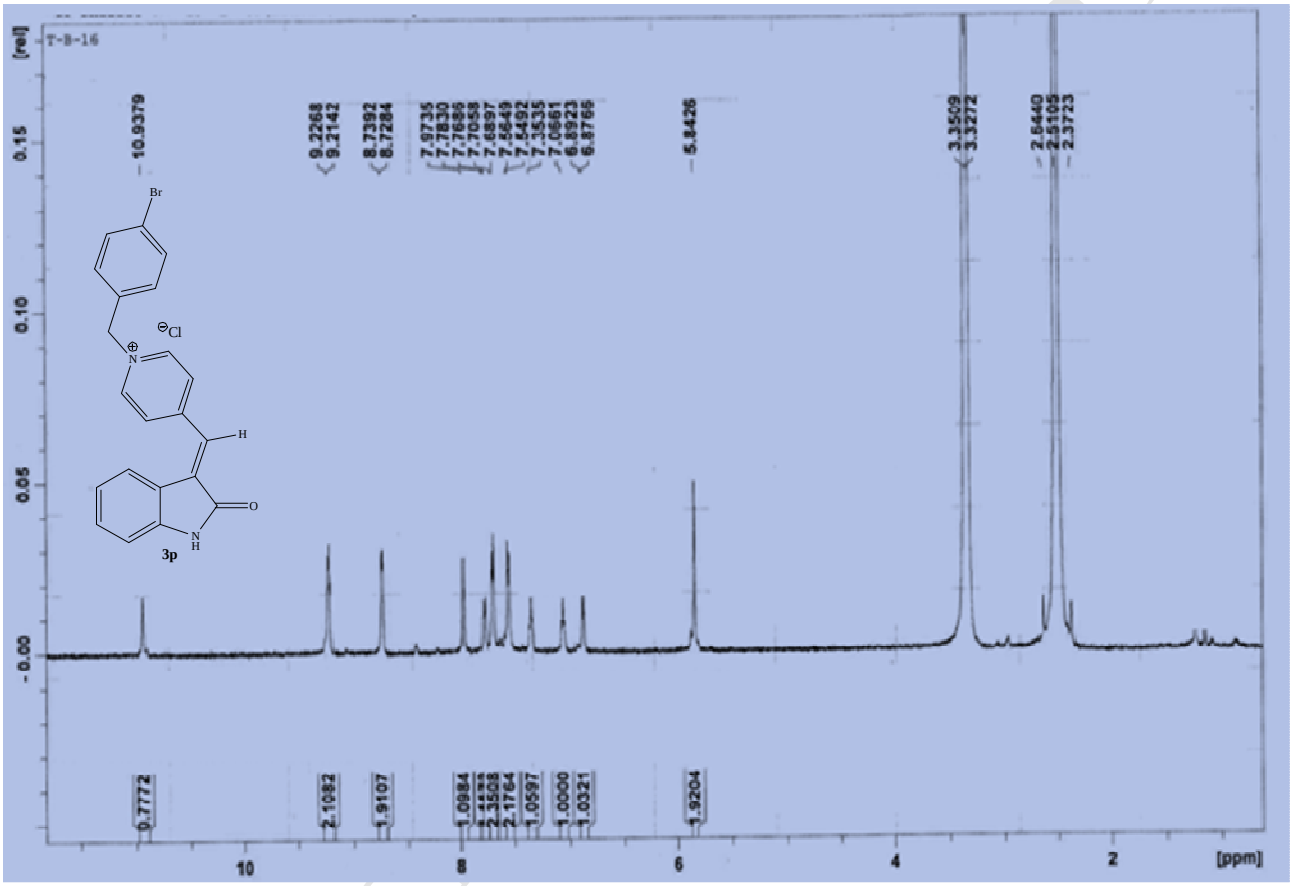
T-B-16
10.9379
9.2268
9.2142
8.7392
8.7284
7.9735
7.7830
7.7686
7.7058
7.6897
7.6449
7.6402
7.3535
7.0661
6.8923
6.8766
5.8426
3.3509
3.3272
2.6449
2.5105
2.3723
Br
Cl
H
O
N
H
3p
0.7772
2.1082
1.9107
1.0984
1.4188
2.3503
2.1764
1.0597
1.0000
1.0321
1.9204
10
8
6
4
2
[ppm]

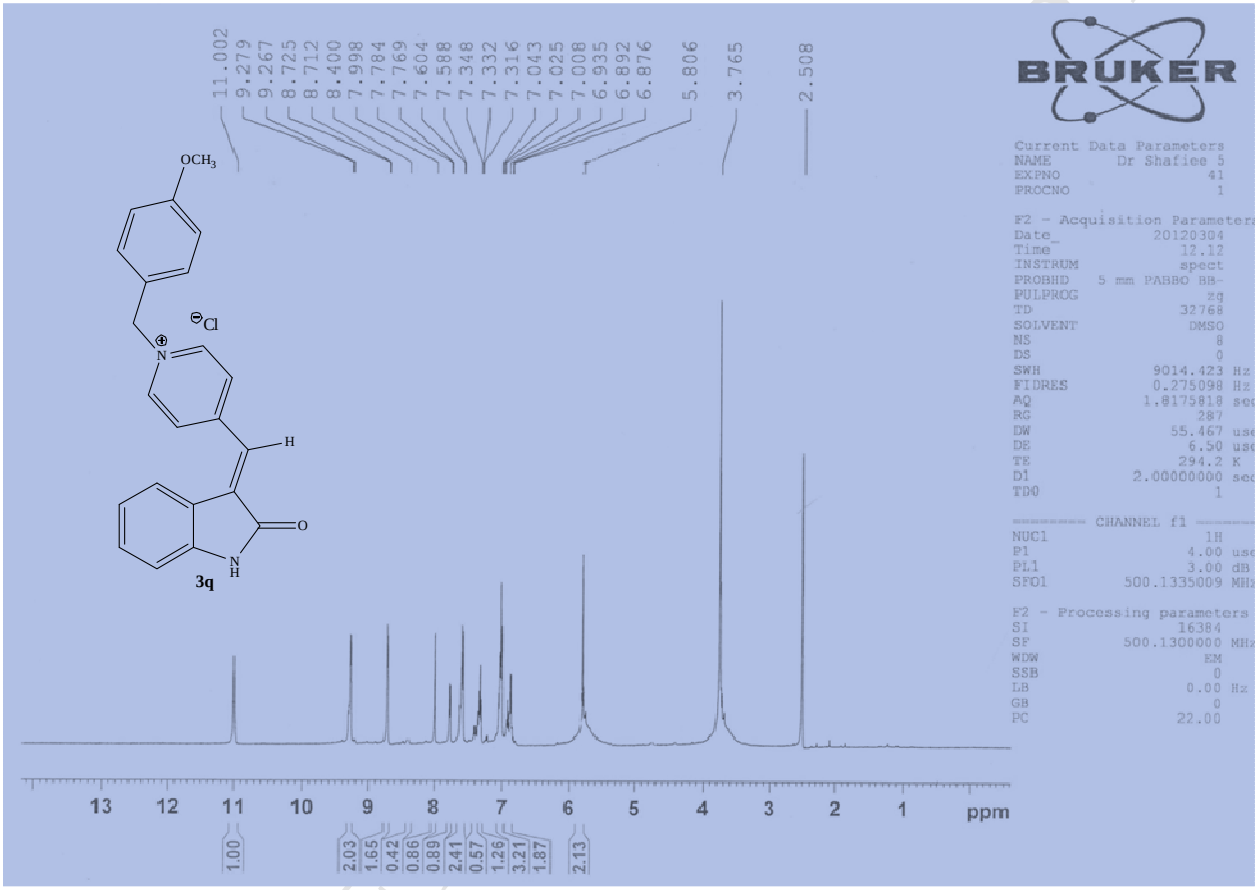
11.002
9.279
9.267
8.725
8.712
8.400
7.998
7.784
7.769
7.604
7.588
7.348
7.332
7.316
7.043
7.025
7.008
6.935
6.892
6.876
5.806
3.765
2.508
OCH3
Cl
N
H
O
N
H
3q
BRUKER
Current Data Parameters
NAME Dr Shafiee 5
EXPNO 41
PROCNO 1
F2 - Acquisition Parameters
Date_ 20120304
Time 12.12
INSTRUM spect
PROBHD 5 mm PABBO BB-
PULPROG zg
TD 32768
SOLVENT DMSO
NS 8
DS 0
SWH 9014.423 Hz
FIDRES 0.275098 Hz
AQ 1.8175818 sec
RG 287
DW 55.467 usec
DE 6.50 usec
TE 294.2 K
D1 2.00000000 sec
TD0 1
CHANNEL f1
NUC1 1H
P1 4.00 usec
PL1 3.00 dB
SFO1 500.1335009 MHz
F2 - Processing parameters
SI 16384
SF 500.1300000 MHz
WDW EM
SSB 0
LB 0.00 Hz
GB 0
PC 22.00
13 12 11 10 9 8 7 6 5 4 3 2 1 ppm
1.00
2.03
1.65
0.42
0.86
0.89
2.41
0.57
1.26
3.21
1.87
2.13

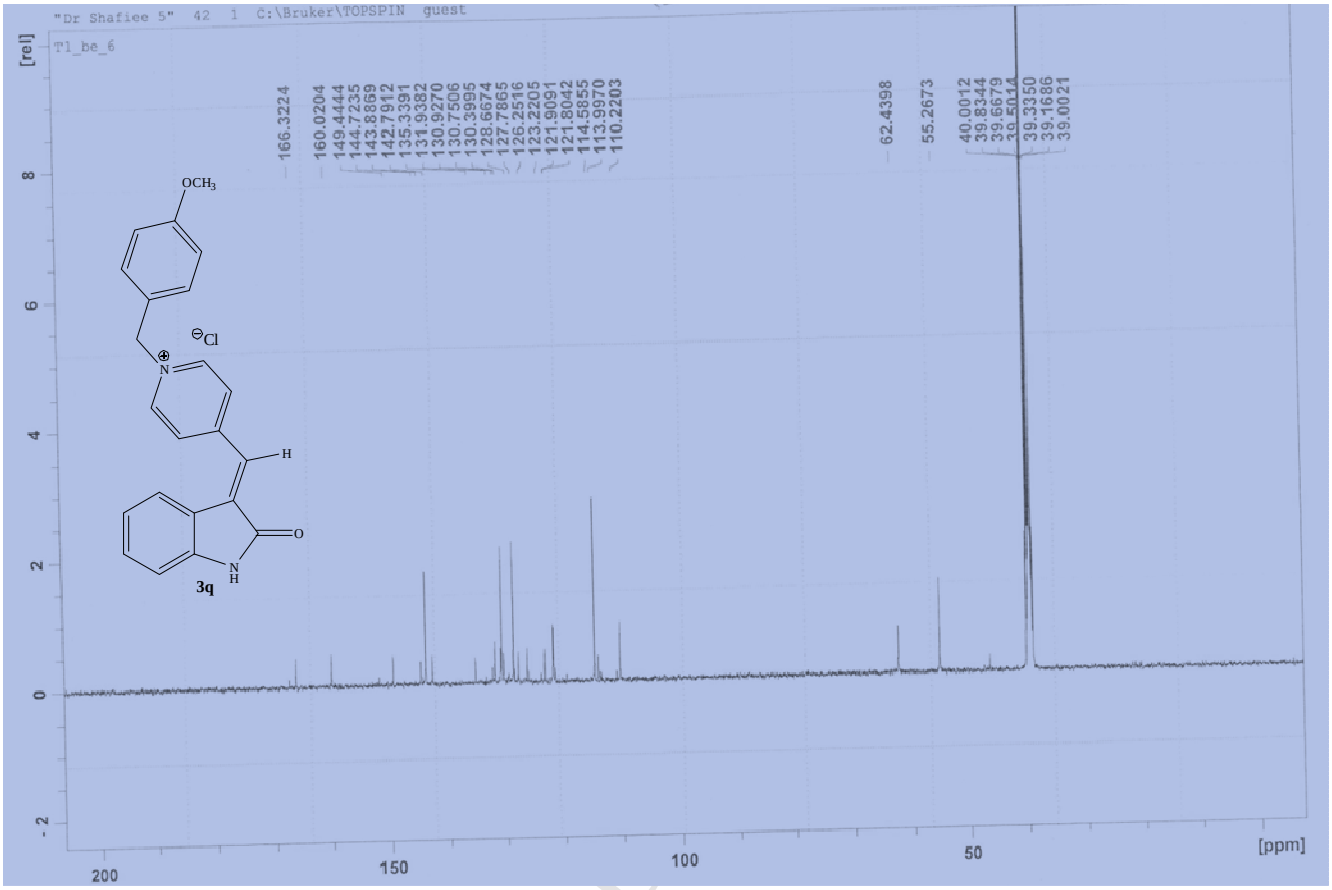

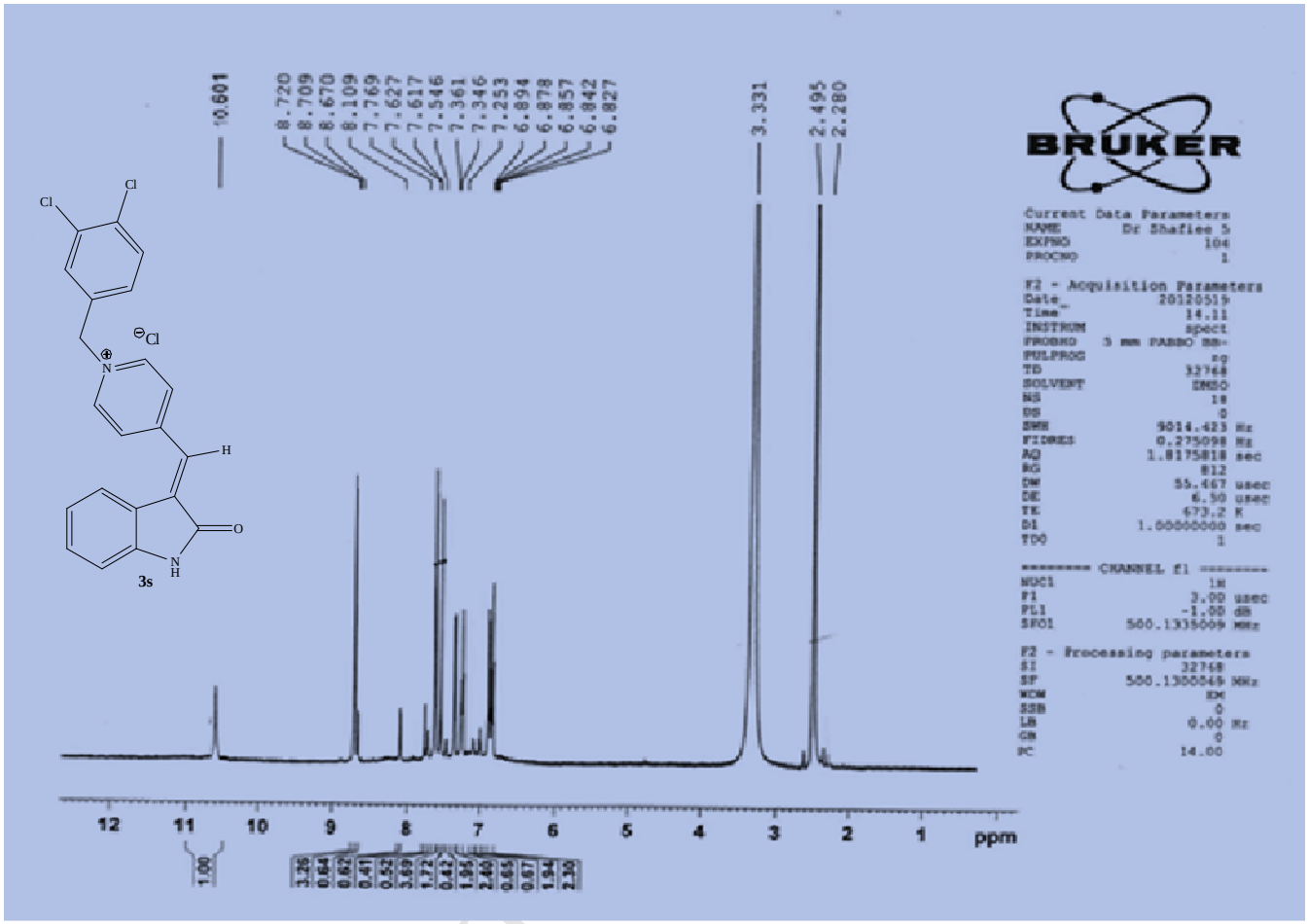

figure 20: ^{1}H NMR (500 MHz, DMSO-d_6) *(Z)-1-(3,4-dichlorobenzyl)-4-((2-oxoindolin-3-ylidene)methyl)pyridinium chloride*

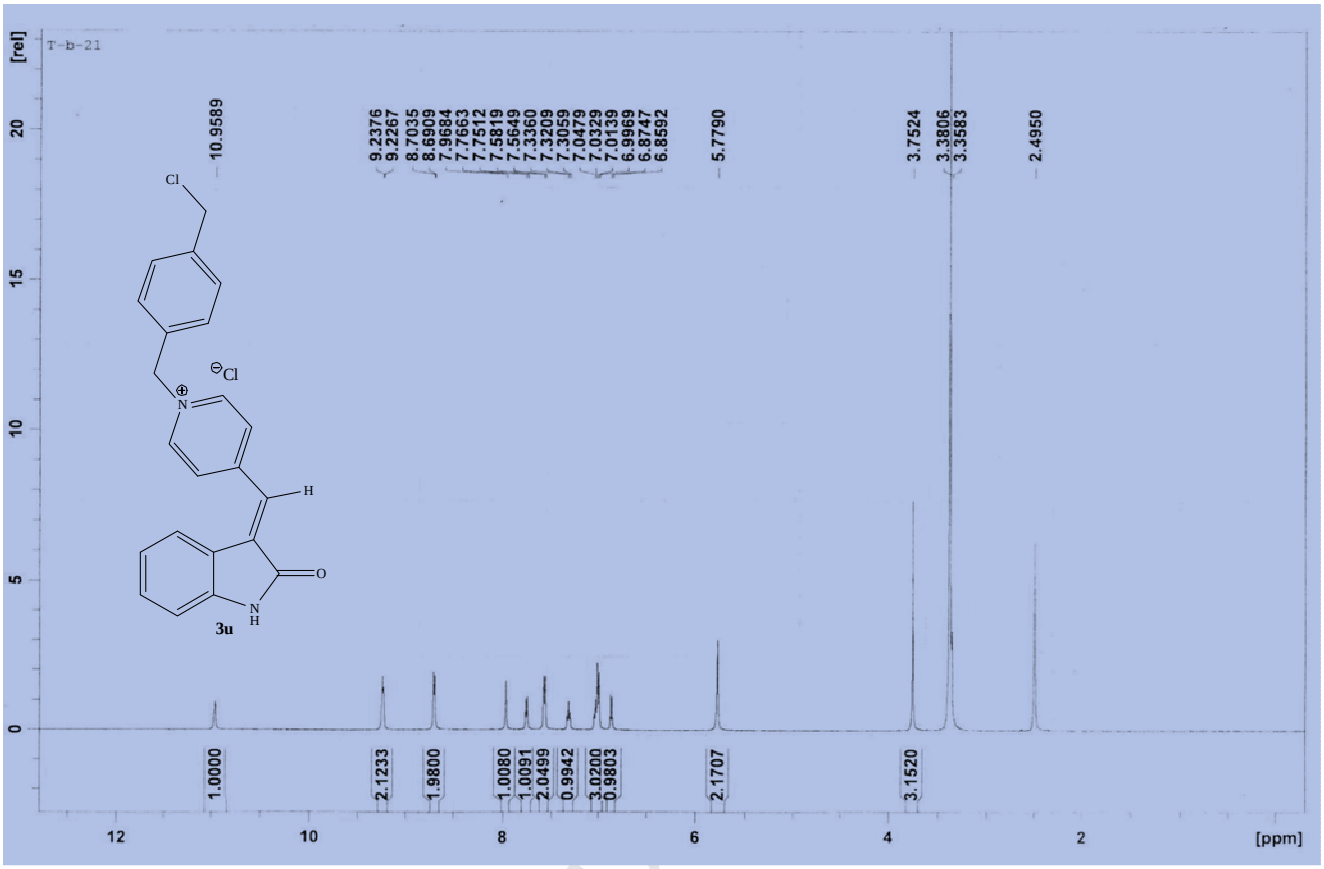
T-b-21
[rel]
20
15
10
5
0
10.9589
9.2376
9.2267
8.7035
8.6909
7.9684
7.7663
7.7512
7.5819
7.5649
7.3360
7.3209
7.3059
7.0479
7.0329
7.0139
6.9969
6.8747
6.8592
5.7790
3.7524
3.3806
3.3583
2.4950
1.0000
2.1233
1.9800
1.0080
1.0091
2.0499
0.9942
3.0200
0.9803
2.1707
3.1520
12
10
8
6
4
2
[ppm]
Cl
⊖Cl
⊕N
H
O
N
H
3u

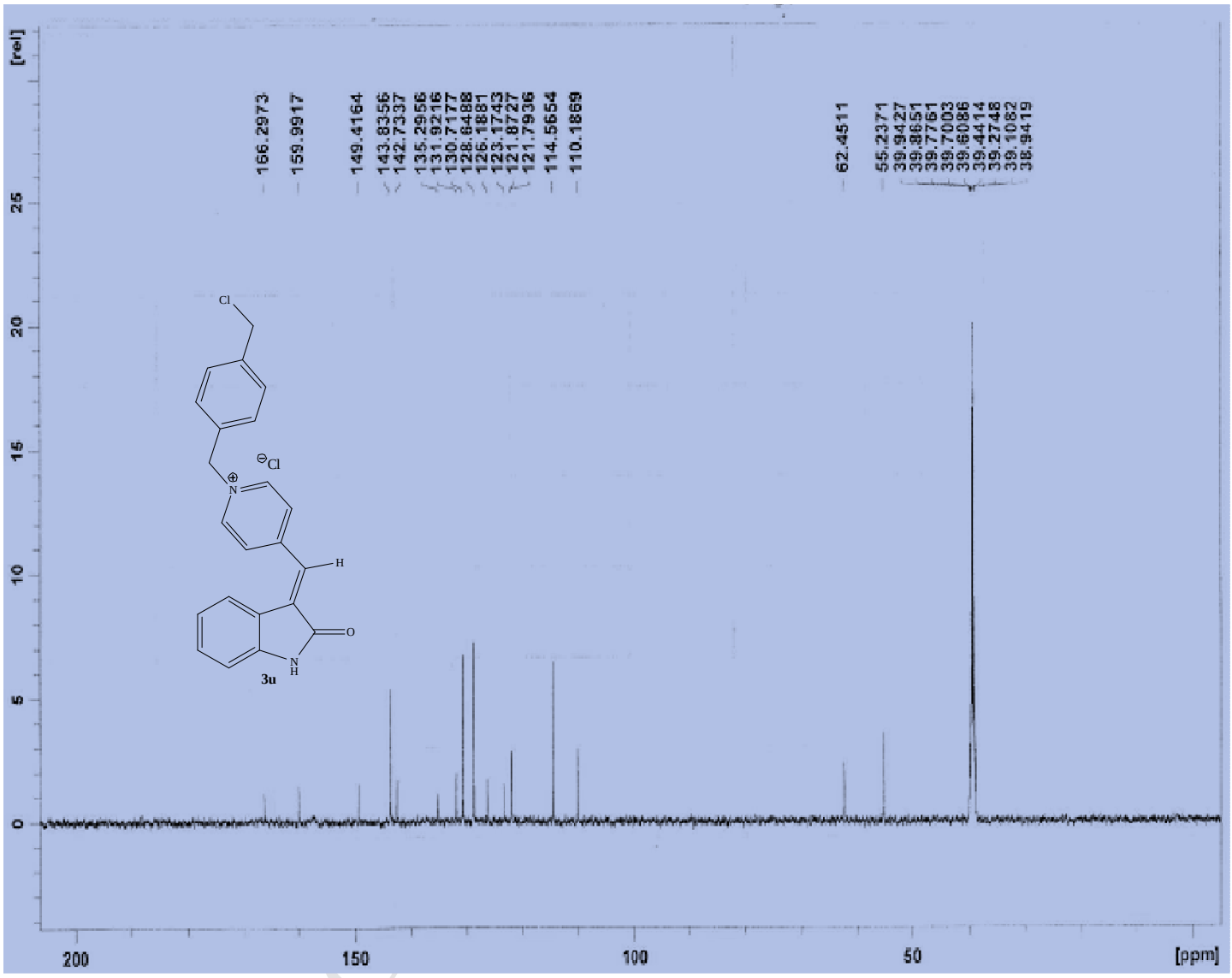
[rel]
25
20
15
10
5
0
166.2973
159.9917
149.4164
143.8356
142.7337
135.2956
131.9216
130.7177
128.8488
126.1881
123.1743
121.8727
121.7936
114.5654
110.1869
62.4511
55.2371
39.9427
39.8651
39.7761
39.7003
39.6086
39.4414
39.2748
39.1082
38.9419
Cl
⊖Cl
N
H
O
N
H
3u
200
150
100
50
[ppm]

Table 3. Predicted ADMET properties of the target compounds **3a-u**.

Compound	BBB penetration		HIA[a] %	Caco-2 Permeability[b]	AMES Toxicity[c]	Acute Toxicity LC_{50}[d] (µmol)
	%	CNS activity				
3a	99	+	99	+	-	2.99
3b	99	+	99	+	-	2.77
3c	99	+	99	+	-	2.71
3d	99	+	99	+	-	2.98
3e	99	+	99	+	-	2.78
3f	88	+	98	+	-	2.65
3g	99	+	99	+	-	2.68
3h	99	+	99	+	-	2.71
3i	99	+	99	+	-	2.71
3j	99	+	99	+	-	2.78
3k	99	+	99	+	-	2.98
3l	99	+	100	+	-	3.15
3m	99	+	99	+	-	2.77
3n	99	+	99	+	-	2.77
3o	99	+	99	+	-	2.71
3p	99	+	99	+	-	2.78
3q	99	+	100	+	-	3.15
3r	91	+	98	+	-	2.66
3s	99	+	99	+	-	2.71
3t	99	+	99	+	-	2.71
3u	99	+	100	+	-	2.87
Donepezil	99	+	99	+	-	3

[a]Human Intestinal Absorption

[b]The values more than **50** was considered as **+**

[c]Mutagenic potential of chemicals

[d]EPA v4b Fathead Minnow Acute Toxicity